Efficient analysis and detection of edges through directional multiscale representations

Kanghui Guo and Demetrio Labate

Abstract The analysis and detection of edges and interface boundaries is a fundamental problem in applied mathematics and image processing. In the study of the wave equation, for example, one is interested in the evolution of moving fronts; in image processing and computer vision, the detection and analysis of edges is an essential task for applications such as shape recognition, image enhancement and classification. Multiscale methods and wavelets have been very successful in this area, due to a combination of useful micro-analytical properties and fast numerical implementations. The continuous wavelet transform in particular, has the ability to signal the location of the singularities of functions and distributions through its asymptotic decay at fine scales. However, this approach is unable to provide additional information about the geometry of the singularity set, such as the edge orientation. This limitation can be overcome by using the continuous shearlet transform, an approach combining the analytical power of multiscale analysis and high directional sensitivity. This chapter gives an overview of the microlocal properties of the shearlet transform and illustrates its ability to provide a precise geometric characterization of edges and interface boundaries in images and other multidimensional data. These results provide the theoretical groundwork for innovative applications in problems of edge detection, feature extraction and geometric separation.

Kanghui Guo
Missouri State University, Springfield, Missouri 65804, USA, e-mail: KanghuiGuo@MissouriState.edu

Demetrio Labate
University of Houston, Houston, Texas 77204, USA, e-mail: dlabate@math.uh.edu

1 Introduction

Edges are prominent features in images. Because they often carry the most important information of an image, analysis and detection of edges is a central topic in image processing, computer vision and pattern recognition.

The first difficulty one encounters is that the concept of 'edge' has both a physical and a visual meaning. In the physical world, edges correspond to discontinuities in the structural, chemical or photometrical properties of real objects. In images, edges are associated with sharp changes of intensity and accurate detection of the locations of these changes is the purpose of edge detection algorithms. In principle, if an image is modelled as a continuous function, sudden intensity changes can be identified by differentiation. However, every realistic image is contaminated by some noise, producing local intensity variations that may confound a naive edge detector scheme based on direct implementation of a differentiation operator. Thus, to design a robust edge detection scheme, more sophisticated algorithmic procedure are usually necessary.

The problem of edge detection is historically intertwined with the modelling of the human visual system. Following the celebrated physiological studies of Golgi, Cajal, Granit, Hartline and others, along with the advent of the modern computer age it emerged the idea that vision is an information processing system, whose first stage works essentially as an edge detector [34]. This idea was articulated most effectively by D. Marr who observed that "the purpose of early visual processing is to construct a primitive but rich description of the image", called a *raw primal sketch* of the image, which is "constructed of the intensity changes in an image, using a primitive language of edge-segments, bars, blobs and terminations" (cf. [34]). Related to this is the fundamental remark that: "A major difficulty with natural images is that changes can and do occur over a wide range of scales. No single filter can be optimal simultaneously at all scales, so it follows that one should seek a way of dealing separately with the changes occurring at different scales." Based on this observation, Marr and Hildreth pioneered the idea of using a multiscale approach to detect edges in images and argued in favour of a method based on the Laplacian of Gaussian (at various scales) inspired by the structure of the receptive field of retinal ganglion cells [35].

In mathematics, edges are usually modelled as discontinuities or, more generally, as singularities of functions and distributions. For example, the two-dimensional Heaviside step function H, given by

$$H(x_1,x_2) = \begin{cases} 1 & \text{if } x_1 > 0, \\ 0 & \text{if } x_1 \leq 0, \end{cases}$$

is a model of an ideal *step edge* in the plane $\mathbb{R}^2$ located along the axis $x_1 = 0$.

The mathematical characterization of step edges and other singularities using multiscale transforms goes back to the origins of the wavelet literature [16] and was inspired in part by the observations from the neurophysiological literature we

described above. In the wavelet approach, the key idea is to construct families of analyzing functions defined over a range of scales and location, that is,

$$\{\psi_{a,t}(x) = a^{-n/2}\psi(a^{-1}(x-t)), \quad a>0, t\in\mathbb{R}^n\},$$

where $\psi \in L^2(\mathbb{R}^n)$ is usually a well-localized function (i.e., it has rapid decay both in the spatial and the Fourier domain). In particular, we can choose ψ such that $\hat{\psi} \in C_c^\infty(\mathbb{R}^n)$ and $\hat{\psi}(0) = 0$. Since ψ has rapid decay in space-domain, the functions $\psi_{a,t}$ are mostly concentrated around t, with the size of the essential support controlled by the scaling parameter a. We can then use these functions to analyze the local regularity of a function or distribution f through the mapping

$$f \to \langle f, \psi_{a,t}\rangle, \quad a>0, t\in\mathbb{R}^n. \tag{1}$$

To illustrate how this approach can be used to identify the location of a step edge, let us apply the transform (1), for $n=2$, to the Heaviside step function H. Using Plancherel theorem, the distributional Fourier transform of H (see Appendix) and denoting $t=(t_1,t_2)\in\mathbb{R}^2$, we have:

$$\begin{aligned}
\langle H, \psi_{a,t}\rangle &= \langle \hat{H}, \hat{\psi}_{a,t}\rangle \\
&= a\int_{\mathbb{R}^2} \hat{H}(\xi_1,\xi_2)\,\overline{\hat{\psi}(a\xi_1,a\xi_2)}\,e^{-2\pi i(\xi_1 t_1+\xi_2 t_2)}\,d\xi_1\,d\xi_2 \\
&= a\int_{\mathbb{R}^2} \frac{\delta_2(\xi_1,\xi_2)}{2\pi i\xi_1}\,\overline{\hat{\psi}(a\xi_1,a\xi_2)}\,e^{-2\pi i(\xi_1 t_1+\xi_2 t_2)}\,d\xi_1\,d\xi_2 \\
&= a\int_{\mathbb{R}} \frac{1}{2\pi i\xi_1}\,\overline{\hat{\psi}(a\xi_1,0)}\,e^{-2\pi i\xi_1 t_1}\,d\xi_1 \\
&= a\int_{\mathbb{R}} \hat{\gamma}(\eta)\,e^{-2\pi i\eta\frac{t_1}{a}}\,d\eta,
\end{aligned}$$

where $\hat{\gamma}(\eta) = \frac{1}{2\pi i\eta}\,\overline{\hat{\psi}(\eta,0)}$. If $t_1=0$, the calculation above shows that $|\langle f,\psi_{a,t}\rangle| \approx a$, provided that $\int_{\mathbb{R}}\hat{\gamma}(\eta)d\eta \neq 0$. On the other hand, if $t_1\neq 0$, an application of the Inverse Fourier Transform theorem yields that $\langle f,\psi_{a,t}\rangle = a\,\gamma(-t_1/a)$. Since $\hat{\gamma}\in C_c^\infty(\mathbb{R})$, γ has rapid decay in space-domain, implying that $\langle H,\psi_{a,t}\rangle$ decays rapidly to 0, as $a\to 0$; that is, for any $N\in\mathbb{N}$, there is a constant $C_N>0$ such that $|\langle H,\psi_{a,t}\rangle| \le C_N a^N$, as $a\to 0$. In summary, *the elements $\langle H,\psi_{a,t}\rangle$ exhibit rapid asymptotic decay, as $a\to 0$, for all $t\in\mathbb{R}^2$ except at the location of the singularity $t_1=0$, where $\langle H,\psi_{a,t}\rangle$ behaves as $O(a)$.*

The mapping $f\to\langle f,\psi_{a,t}\rangle$ is the classical *continuous wavelet transform* and the above example illustrates its ability to characterize the location of the discontinuities of f through its asymptotic decay at fine scales. More generally, the continuous wavelet transform can be used to characterize the singular support of a distribution, that is, the set of points where it fails to be regular [27, 36], and to measure its local regularity [29, 30].

However, despite the remarkable ability of the continuous wavelet transform in resolving the local regularity of a function of distribution, this approach is very

limited in terms of extracting the *geometry* of the singularity set. In the example of the Heaviside step function H, for instance, the continuous wavelet transform detects the *location* of edge points but provides no information about the *orientation* of the singularity line. In dimensions two and higher, when the singularity points are supported on a curve or a higher dimensional manifold, it is useful not only to detect the location of the singularity points but also to capture the geometry of the singularity set. In the language of microlocal analysis, we want to detect not only the singular support of a distribution, but also its wavefront set.

In the mathematical literature, the idea of using wavelet-like transforms to perform microlocal analysis can be traced back to Bros and Iagolnitzer [1] and Cordoba and Fefferman [5], who both defined transforms with implicitly a kind of anisotropic scaling and used these transforms to address various questions in microlocal analysis. It was later shown that the Fourier-Bros-Iagolnitzer (FBI) transform is able to resolve not only the singular support but also the wavefront set of a distribution [9, 14]. During the last decade, with the introduction of a new generation of directional multiscale systems in the wavelet literature, most notably the curvelet [3] and shearlet systems [18], it was shown that it is possible to define 'generalized' wavelet transforms able to resolve the wavefront set of distributions [4, 15, 31]. Among such transforms, the *continuous shearlet transform* offers an especially appealing mathematical framework, due to a simple construction, derived from the general setting of affine systems, and its high directional sensitivity obtained through the action of anisotropic dilations and shear transformations. One major advantage of this approach is that, thanks to the affine structure, there is a rather direct procedure to derive discrete versions of the shearlet transform and transfer the theoretical properties of the continuous transform to its discrete counterparts. This property is especially useful for image processing and other numerical applications.

In this chapter, we present a review of the mathematical results concerning the application of the *continuous shearlet transform* to the analysis and detection of edge-type singularities in multivariate functions and distributions. As we will show below, the continuous shearlet transform enables a precise geometric characterization of edges and other singularity sets in multivariate functions and distributions. For instance, in the case of the two-dimensional Heaviside step function, the continuous shearlet transform characterizes both the location and the orientation of the discontinuity line. More generally, it can be used to identify the geometry of curvilinear edges and detect corner points in functions of two variables and similarly to characterize surface boundaries, wedges and corner points in functions of three variables.

The rest of the chapter is organize as follows. In Section 2, we recall the definition of the continuous wavelet and shearlet transforms. In Section 3, we present the shearlet analysis of step discontinuities in the two-dimensional case. The main theorem we prove is a generalization of results previously appeared in the literature and shows that the shearlet-based analysis can be used not only to detect the location and orientation of an edge, but also to extract information about its curvature. In Section 4, we discuss the extension of the shearlet analysis of step discontinuities to the three-dimensional case. We make some additional remarks about the

analysis of other types of edge singularities in Section 5, where we also include a brief survey of the numerical applications of the results discussed in this chapter. In the Appendix, we collect some basic definitions and results about Fourier analysis, including Fourier analysis of distributions.

2 The continuous wavelet transform and its generalizations

In this section, we recall the definition of the continuous wavelet transform, first in dimension one and then in higher dimensions. We define the continuous shearlet transform within this setting as a special realization of the continuous wavelet transform in dimensions $n \geq 1$.

2.1 Continuous wavelets

The *affine group* associated with $\mathbb{R}$, denoted by $\mathscr{A}$, consists of all pairs

$$(a,t) \in \mathbb{R}_+ \times \mathbb{R}$$

with the group operation

$$(a,t)\cdot(a',t') = (aa', at'+t).$$

This operation is consistent with the action of $g = (a,t) \in \mathscr{A}$ on $x \in \mathbb{R}$ given by $g(x) = ax+t$. Note that $g^{-1} = (a,t)^{-1} = (a^{-1}, a^{-1} - a^{-1}t)$. For $\psi \in L^2(\mathbb{R})$, a unitary representation of $\mathscr{A}$ acting on $L^2(\mathbb{R})$ is the mapping $\pi : \mathscr{A} \mapsto \mathscr{U}(L^2(\mathbb{R}))$ given by

$$(\pi(a,t)\psi)(x) = a^{-1/2}\psi((a,t)^{-1}x) = a^{-1/2}\psi(a^{-1}(x-t)) := \psi_{a,t}(x),$$

where $\mathscr{U}(L^2(\mathbb{R}))$ denotes the group of unitary representations on $L^2(\mathbb{R}^2)$. The collection of functions

$$\{\psi_{a,t} : (a,t) \in \mathscr{A}\}$$

is called a *continuous wavelet system* generated by $\psi \in L^2(\mathbb{R}^2)$ and the mapping $\mathscr{W}_\psi$ taking $f \in L^2(\mathbb{R})$ into the function

$$\mathscr{W}_\psi f(a,t) = \langle f, \psi_{a,t}\rangle = a^{-1/2}\int_{\mathbb{R}} f(x)\,\overline{\psi(a^{-1}(x-t))}\,dx \tag{2}$$

on $\mathscr{A}$ is the *continuous wavelet transform* of f.

One major goal of wavelet theory is to find conditions on ψ so that one can reconstruct f from its wavelet transform via the reproducing formula

$$f = \int_{\mathscr{A}} \langle f, \psi_{a,t}\rangle\, \psi_{a,t}\, d\lambda(a,t), \tag{3}$$

where $d\lambda(a,t) = a^{-2}dadt$ is the left Haar measure on $\mathscr{A}$ and the equality is understood in the weak sense. This condition, called *admissibility condition*, was discovered by Calderòn [2] and is given by the expression

$$\int_0^\infty |\hat{\psi}(a\xi)|^2 \frac{da}{a} = 1, \quad \text{for a.e. } \xi \in \mathbb{R}. \tag{4}$$

An admissible function ψ satisfying the reproducing formula (3) is called a *continuous wavelet* on $\mathscr{A}$. Clearly, there are many examples of continuous wavelets on $\mathscr{A}$, as one can choose any $\psi \in L^2(\mathbb{R})$ such that $\hat{\psi}$ is a bounded function supported in a compact set in $\mathbb{R} \setminus \{0\}$.

The extension of the notion of continuous wavelet and continuous wavelet transform to n dimensions follows along the same lines presented above, once we replace the affine group with its multi-dimensional version. The *full affine group of motions* on $\mathbb{R}^n$, denoted by $\mathscr{A}_n$, consists of all pairs $(M,t) \in GL_n(\mathbb{R}) \times \mathbb{R}^n$ with group operation

$$(M,t)\cdot(M',t') = (MM', Mt'+t).$$

This operation is associated with the action $x \mapsto Mx+t$ on $\mathbb{R}^n$.

We consider the subgroups $\Lambda = \{(M,t) : M \in G, t \in \mathbb{R}^n\} \subset \mathscr{A}_n$, where G is a closed subgroup of $GL_2(\mathbb{R})$. We can identify G with the subgroup $\{(M,t) \in \Lambda : M \in G, t = 0\}$ and we refer to it as the *dilation subgroup* of Λ. Similarly, we refer to the subgroup $N = \{(M,t) \in \Lambda : M = I, t \in \mathbb{R}^n\}$ as the *translation subgroup* of Λ. For $\psi \in L^2(\mathbb{R}^2)$, a unitary representation of Λ acting on $L^2(\mathbb{R}^2)$ is defined by

$$(\rho(M,t)\psi)(x) = |\det M|^{-\frac{1}{2}} \psi(M^{-1}(x-t)) := \psi_{M,t}(x).$$

Then, similar to the one-dimensional case, a continuous wavelet system generated by $\psi \in L^2(\mathbb{R}^2)$ is a collection of functions of the form

$$\left\{ \psi_{M,t}(x) = |\det M|^{-\frac{1}{2}} \psi(M^{-1}(x-t)) : \ (M,t) \in \Lambda \right\}$$

and the mapping $\mathscr{W}_\psi$ taking $f \in L^2(\mathbb{R}^n)$ into the function

$$\mathscr{W}_\psi f(M,t) = \langle f, \psi_{M,t} \rangle = |\det M|^{-1/2} \int_{\mathbb{R}^n} f(x) \, \overline{\psi(M^{-1}(x-t))} \, dx \tag{5}$$

is the *continuous wavelet transform* of f on Λ associated with $\psi \in L^2(\mathbb{R}^n)$. Similar to the one-dimensional case, a function $\psi \in L^2(\mathbb{R}^n)$ is said to be admissible and is called a *continuous wavelet* on Λ if any $f \in L^2(\mathbb{R}^n)$ can be recovered via the reproducing formula

$$f = \int_\Lambda \langle f, \psi_{M,t} \rangle \, \psi_{M,t} \, d\lambda(M,t), \tag{6}$$

where λ is the left Haar measure for Λ and, as above, the equality is understood in the weak sense. We write $d\lambda(M,t) = d\mu(M)dt$, where μ is the left Haar measure of G. The following proposition gives the admissibility condition for a function ψ

satisfying formula (6). The proof that we include is taken from [31] and it follows the main ideas from [40].

Proposition 1. *Equality (6) is valid for all $f \in L^2(\mathbb{R}^n)$ if and only if*

$$\Delta(\psi)(\xi) = \int_G |\hat{\psi}(\xi M)|^2 \, |\det M| \, d\mu(M) = 1, \tag{7}$$

for all $\xi \in \mathbb{R}^n \setminus \{0\}$.

Proof. Suppose that (7) holds. Given any $f \in L^2(\mathbb{R}^n)$, an application of Parseval and Plancherel formulas yields:

$$\begin{aligned}
\|\mathscr{W}_\psi f\|^2_{L^2(\Lambda)} &= \int_{\mathbb{R}^n} \int_G |\langle f, \psi_{M,t}\rangle|^2 \, d\mu(M)\, dt \\
&= \int_{\mathbb{R}^n} \int_G \left| \int_{\mathbb{R}^n} \hat{f}(\xi)\, \overline{\hat{\psi}(\xi M)}\, e^{2\pi i \xi t} d\xi \right|^2 |\det M| \, d\mu(M)\, dt \\
&= \int_{\mathbb{R}^n} \int_G \left| \left(\hat{f}\, \overline{\hat{\psi}(\cdot M)} \right)^\vee (t) \right|^2 |\det M| \, d\mu(M)\, dt \\
&= \int_G \int_{\mathbb{R}^n} \left| \left(\hat{f}\, \overline{\hat{\psi}(\cdot M)} \right)^\vee (t) \right|^2 dt \, |\det M| \, d\mu(M) \\
&= \int_G \int_{\mathbb{R}^n} |\hat{f}(\xi)|^2 \, |\hat{\psi}(\xi M)|^2 \, |\det M| \, d\xi \, d\mu(M) \\
&= \int_G |\hat{f}(\xi)|^2 \, \Delta(\psi)(\xi)\, d\xi = \|f\|^2_{L^2(\mathbb{R}^n)}.
\end{aligned}$$

This shows that the mapping

$$\mathscr{W}_\psi : L^2(\mathbb{R}^n) \to L^2(\Lambda)$$

is an isometry. By polarization we thus have that

$$\langle \mathscr{W}_\psi f, \mathscr{W}_\psi g \rangle_{L^2(\Lambda)} = \langle f, g \rangle_{L^2(\mathbb{R}^n)}$$

for all f, f in $L^2(\mathbb{R}^n)$ giving equation (6).

Conversely, suppose that

$$\int_{\mathbb{R}^n} \int_G |\langle f, \psi_{M,t}\rangle|^2 \, d\mu(M)\, dt = \|f\|^2$$

for all $f \in L^2(\mathbb{R}^n)$. Let ξ_0 be a point of differentiability of $\Delta(\psi)(\xi)$ and let $\hat{f}(\xi) = |B(\xi_0, r)|^{-1/2} \chi_{B(\xi_0,r)}(\xi)$, where $B(\xi_0, r)$ is a ball centered at ξ_0 of radius r. By reversing the chain of equalities above we conclude that

$$\frac{1}{|B(\xi_0, r)|} \int_{B(\xi_0,r)} \Delta(\psi)(\xi)\, d\xi = 1$$

for all $r > 0$. Letting $r \to 0$, we obtain that $\Delta(\psi)(\xi_0) = 1$, and, since almost each $\xi \in \mathbb{R}^n$ is a point of differentiability, (7) holds. □

If G is the affine group $\mathscr{A}$, then $|\det a| = a$, $d\mu(a) = \frac{da}{a}^2$ and (7) gives the classical Calderòn condition (4). Also, note that Proposition 2 can be extended to the situation where Λ is just a subset and not a subgroup of $\mathscr{A}_n$.

For a given dilations group G, it does not always exist an admissible function ψ for which the reproducing formula (6) holds. For example, it is not difficult to show that the group of 2×2 orthogonal matrices $SO(2)$ acting on $\mathbb{R}^2$ is not associated to any admissible ψ. We refer the interested reader to [33, 40] for an illuminating discussion about the admissible dilation groups and several related results.

The simplest example of dilation group we can consider is $G = \{aI_n : a > 0\}$, where I_n is the $n \times n$ identity matrix. In this case, similar to the one-dimensional case (5), we can choose as admissible function any $\psi \in L^2(\mathbb{R})$ such that $\hat{\psi}$ is a bounded function supported in a compact set in $\mathbb{R}^n \setminus \{0\}$. This choice of dilation group is associated with *isotropic* dilations since the action of an element of the group $(aI_n, t) \in \Lambda$ on $x \in \mathbb{R}^n$ is given by $ax + t$ where the same dilation factor a is applied to each coordinate direction. It is reasonable to expect that for more general dilation groups G we can obtain wavelet transforms with more interesting geometric properties. This can achieved, in particular, using a special subgroup of upper triangular matrices in $GL(n, \mathbb{R})$ associated with the so-called shearlet group as will be shown in the next section.

2.2 Continuous shearlets

The *shearlet group*, originally introduced in [7, 31], is the subgroup $\mathbb{S}$ of $\Lambda \subset GL(n, \mathbb{R})$ where, for a fixed parameter $\beta = (\beta_1, \ldots, \beta_{n-1}) \in \mathbb{R}^{n-1}$, the dilation group G consists of the matrices

$$M(a,s) = \begin{pmatrix} a & -a^{\beta_1} s_1 & \ldots & -a^{\beta_{n-1}} s_{n-1} \\ 0 & a^{\beta_1} & \ldots & 0 \\ \vdots & \vdots & \vdots & \vdots \\ 0 & 0 & \ldots & a^{\beta_{n-1}} \end{pmatrix},$$

with $a > 0$ and $s = (s_1, \ldots, s_{n-1}) \in \mathbb{R}^{n-1}$. Usually the parameters β_i are chosen so that $0 < \beta_i < 1$, for all $1 \leq i < n$, as this ensures useful geometric properties for the functions generated under the action of this group. For example, in [8] all β_i are chosen to be equal to $1/n$, as this generalizes the parabolic scaling condition (see further comments in the next section).

We observe that the matrix $M(a,s)$ can be written as the product $B(s)A(a)$ of the *anisotropic dilation matrix*

$$A(a) = \begin{pmatrix} a & 0 & \dots & 0 \\ 0 & a^{\beta_1} & \dots & 0 \\ \vdots & \vdots & \vdots & \vdots \\ 0 & 0 & \dots & a^{\beta_{n-1}} \end{pmatrix}$$

and the *shear matrix*

$$B(s) = \begin{pmatrix} 1 & -s_1 & \dots & -s_{n-1} \\ 0 & 1 & \dots & 0 \\ \vdots & \vdots & \vdots & \vdots \\ 0 & 0 & \dots & 1 \end{pmatrix}.$$

Hence, the action of $(M(a,s),t) \in \mathbb{S}$ on $x \in \mathbb{R}^n$ is given by $M(a,s)x+t = B(s)A(a)x+t$. This shows that each coordinate x_i of x is multiplied by different dilation factor $a^{\beta_{i-1}}$ and this operation is followed by the multiplication by the non-expanding matrix $B(s)$.

For $\psi \in L^2(\mathbb{R}^n)$, the shearlet representation acting on $L^2(\mathbb{R}^n)$ is the unitary representation defined by

$$(\rho(M(a,s),t)\psi)(x) = |\det M(a,s)|^{-\frac{1}{2}} \psi(M(a,s)^{-1}(x-t)) := \psi_{M(a,s),t}(x)$$

and a *continuous shearlet system* is a collection of functions of the form

$$\{\psi_{M(a,s),t}(x) = |\det M(a,s)|^{-\frac{1}{2}} \psi(M(a,s)^{-1}(x-t)) : (M(a,s),t) \in \mathbb{S}\}.$$

The mapping $\mathscr{SH}_\psi$ taking $f \in L^2(\mathbb{R}^n)$ into the function

$$\mathscr{SH}_\psi f(M(a,s),t) = \langle f, \psi_{M(a,s),t} \rangle = |\det M(a,s)|^{-\frac{1}{2}} \int_{\mathbb{R}^n} f(x)\, \overline{\psi(M(a,s)^{-1}(x-t))}\, dx$$

is the *continuous shearlet transform* of f associated with $\psi \in L^2(\mathbb{R}^n)$.

It is not difficult to see that there exist admissible functions $\psi \in L^2(\mathbb{R}^n)$ such that any $f \in L^2(\mathbb{R}^n)$ can be recovered from the reproducing formula

$$f = \int_{\mathbb{S}} \langle f, \psi_{M(a,s),t} \rangle\, \psi_{M(a,s),t}\, d\lambda(M(a,s),t),$$

where λ is the left Haar measure for $\mathbb{S}$. It is a rather simple calculation to show that $d\lambda(M(a,s),t) = \frac{da}{a^3} dsdt$. We will show examples of admissible functions in the next section, where we illustrate the properties of shearlet systems in dimension $n = 2$.

We refer the interested reader to [6] for a more detailed discussion of the shearlet group and its connection with the extended Heisenberg groups and the subgroups of the symplectic group.

2.3 Continuous shearlets in the plane ($n = 2$)

We now examine in more detail the properties of continuous shearlets in dimension $n = 2$.

In accord with the general setting defined in the section above, for a fixed $0 < \beta < 1$, a continuous shearlet system generated by $\psi \in L^2(\mathbb{R}^2)$ is a collection of functions

$$\{\psi_{a,s,t}(x) = |\det M(a,s)|^{-\frac{1}{2}} \psi(M(a,s)^{-1}(x-t)) : a > 0, s \in \mathbb{R}, t \in \mathbb{R}^2\}, \quad (8)$$

where $M(a,s) = \begin{pmatrix} a & -a^\beta s \\ 0 & a^\beta \end{pmatrix}$. As in the general case, we can write $M(a,s) = B(s)A(a)$, where $A(a) = \begin{pmatrix} a & 0 \\ 0 & a^\beta \end{pmatrix}$ and $B(s) = \begin{pmatrix} 1 & -s \\ 0 & 1 \end{pmatrix}$. When $\beta = \frac{1}{2}$, the anisotropic dilation matrix $A(a)$ is associated with the so-called *parabolic scaling*, meaning that the action of the matrix on an element of $\mathbb{R}^2$ produces a scaling that, along one coordinate axis, is quadratic with respect to the other coordinate direction. Parabolic scaling is especially relevant in the construction of discrete systems of curvelets and shearlets since it plays a critical role in ensuring that such system satisfy nearly optimal approximation properties for functions in class of cartoon-like images (cf. [3, 18]).

To obtain an admissible function $\psi \in L^2(\mathbb{R})$ for the shearlet system (8), we define ψ in the Fourier domain as

$$\hat{\psi}(\xi_1, \xi_2) = \hat{\psi}_1(\xi_1)\, \hat{\psi}_2(\tfrac{\xi_2}{\xi_1}),$$

where

$$\int_0^\infty |\hat{\psi}_1(a\omega)|^2 \frac{da}{a} = 1, \text{ for a.e. } \omega \in \mathbb{R}; \quad \|\psi_2\|_2 = 1. \quad (9)$$

We have the following result from [31].

Proposition 2. *Let ψ be chosen as above, with $\hat{\psi}_1$ and $\hat{\psi}_2$ satisfying* (9)*. Any $f \in L^2(\mathbb{R}^2)$ satisfies*

$$f = \int_{\mathbb{R}^2} \int_{\mathbb{R}} \int_0^\infty \langle f, \psi_{a,s,t} \rangle\, \psi_{a,s,t}\, \frac{da}{a^3}\, ds\, dt, \quad (10)$$

where the equality is understood in the L^2 sense.

Proof. To prove the proposition, it is sufficient to show that the admissibility condition (7) from Proposition 2 is satisfied for $M = M(a,s)$.

Observing that $(\xi_1, \xi_2)M = (a\xi_1, a^\beta(\xi_2 - s\xi_1))$ and that $d\lambda(M(a,s),t) = d\mu(M(a,s))dt = a^{-3} da ds dt$, then the admissibility condition (7) becomes

$$\Delta(\psi)(\xi) = \int_{\mathbb{R}} \int_0^\infty |\hat{\psi}_1(a\xi_1)|^2\, |\hat{\psi}_2(a^{\beta-1}(\tfrac{\xi_2}{\xi_1} - s))|^2\, a^{1+\beta} \frac{da}{a^3}\, ds = 1. \quad (11)$$

Using the assumptions on ψ_1 and ψ_2, we finally have that

$$\begin{aligned}\Delta(\psi)(\xi) &= \int_{\mathbb{R}}\int_{\mathbb{R}^+} |\hat{\psi}_1(a\,\xi_1)|^2\,|\hat{\psi}_2(a^{\beta-1}(\tfrac{\xi_2}{\xi_1}-s))|^2\,a^{\beta-2}da\,ds \\ &= \int_{\mathbb{R}^+} |\hat{\psi}_1(a\,\xi_1)|^2 \left(\int_{\mathbb{R}} |\hat{\psi}_2(a^{\beta-1}\,\tfrac{\xi_2}{\xi_1}-s)|^2\,ds\right)\frac{da}{a} \\ &= \int_{\mathbb{R}^+} |\hat{\psi}_1(a\,\xi_1)|^2\,\frac{da}{a} = 1 \quad \text{for a.e. } \xi=(\xi_1,\xi_2)\in\mathbb{R}^2.\end{aligned}$$

This shows that equality (11) is satisfied and, hence, ψ is an admissible function for the shearlet system. □

In many cases, including the applications we will consider in the following, some additional assumptions are required on the functions ψ_1, ψ_2. Namely, both functions are assumed to be C_c^∞ in the Fourier domain with

$$\operatorname{supp}\hat{\psi}_1 \subset [-2,-\frac{1}{2}]\cup[\frac{1}{2},2]$$

and

$$\operatorname{supp}\hat{\psi}_1 \subset [-1,1].$$

The elements of the shearlet system can be written in the Fourier domain as:

$$\hat{\psi}_{a,s,t}(\xi_1,\xi_2) = a^{\frac{1+\beta}{2}}\,\hat{\psi}_1(a\,\xi_1)\,\hat{\psi}_2(a^{\beta-1}(\tfrac{\xi_2}{\xi_1}-s))\,e^{-2\pi i\xi\cdot t}.$$

Thus, by the assumptions on ψ_1 and ψ_2, it follows that the functions $\hat{\psi}_{a,s,t}$ have supports:

$$\operatorname{supp}\hat{\psi}_{a,s,t} \subset \{(\xi_1,\xi_2) : \xi_1\in[-\tfrac{2}{a},-\tfrac{1}{2a}]\cup[\tfrac{1}{2a},\tfrac{2}{a}],\ |\tfrac{\xi_2}{\xi_1}-s|\le a^{1-\beta}\}.$$

That is, the support of $\hat{\psi}_{a,s,t}$ is a pair of trapezoids, symmetric with respect to the origin, oriented along a line of slope s. The trapezoidal supports becomes increasingly more elongated as $a\to 0$. Note that, since the functions $\hat{\psi}_{a,s,t}$ are in C_c^∞, in space domain the elements $\psi_{a,s,t}$ are well localized (even though, clearly, not compactly supported), and their essential support is also highly anisotropic with orientation controlled by s. In summary, the elements of a continuous shearlet system form a collection of well-localized functions ranging over a multitude of scales, orientations and locations, associated with the variable a, s and t, respectively.

Some representative support sets of the functions $\hat{\psi}_{a,s,t}$ are illustrated in Fig. 1.

Even though the continuous shearlet systems (8) exhibit directionality properties going beyond the traditional isotropic wavelet systems, they do have a directional bias which is a consequence of the fact that shear variable s is associated with the slope and not the rotation angle [1] In fact, to produce a shearlet function aligned with the vertical axis, the shear variable s need to increase asymptotically up to ∞.

[1] Clearly one could try to define a wavelet-like system using dilations and rotations rather than dilations and shear, like we are describing here. This is what is done by the curvelet approach. One disadvantage, in the curvelet case, it that one looses the group structure inherited by the theory of affine systems.

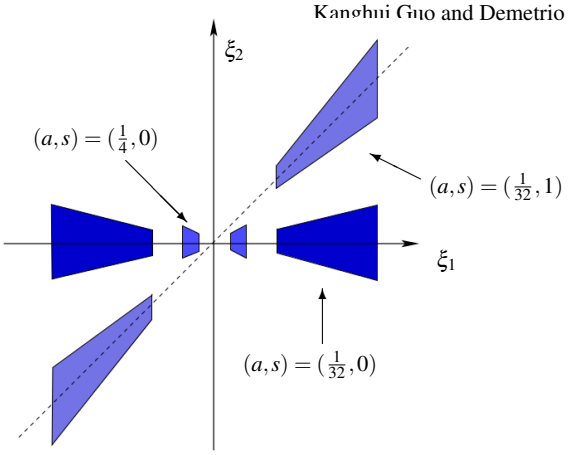

Fig. 1 Fourier domain supports of representative elements $\psi_{a,s,t}$ of a continuous shearlet system, for different values of a and s.

It follows that, if a function f is mostly concentrated along the vertical axis in the Fourier domain, the energy of f will be mostly concentrated in the components of the continuous shearlet transform $\mathscr{SH}_\psi f(M(a,s),t)$ as $s \to \infty$.

The standard way to address this problem is to modify the continuous shearlet systems (8) as follows. Rather than letting the shear variable s to be defined over $\mathbb{R}$, its range is restricted to an interval, for example $s \in [0,2]$. Under this restriction, the continuous shearlet system does not satisfy the reproducing formula (10) since the values of s only cover the set of orientations contained in a cone-region centered along the horizontal axis in the Fourier domain (see Fig. 1). The remaining set of orientations will now be handled by a second continuous shearlet system.

More precisely, let $\psi^{(h)}, \psi^{(v)} \in L^2(\mathbb{R}^2)$ be given by

$$\hat{\psi}^{(h)}(\xi_1,\xi_2) = \hat{\psi}_1(\xi_1)\,\hat{\psi}_2(\tfrac{\xi_2}{\xi_1}), \quad \hat{\psi}^{(v)}(\xi_1,\xi_2) = \hat{\psi}_1(\xi_2)\,\hat{\psi}_2(\tfrac{\xi_1}{\xi_2}),$$

and, for a fixed $0<\beta<1$, let $N(a,s) = \begin{pmatrix} a^\beta & 0 \\ -a^\beta s & a \end{pmatrix}$. We define the *horizontal* and *vertical continuous shearlets* by

$$\psi^{(h)}_{a,s,t}(x) = |\det M(a,s)|^{-\frac{1}{2}}\,\psi^{(h)}(M(a,s)^{-1}(x-t)), \quad a>0, s\in\mathbb{R}, t\in\mathbb{R}^2,$$

and

$$\psi^{(v)}_{a,s,t}(x) = |\det N(a,s)|^{-\frac{1}{2}}\,\psi^{(v)}(N(a,s)^{-1}(x-t)), \quad a>0, s\in\mathbb{R}, t\in\mathbb{R}^2,$$

respectively.

For $0<a<\frac{1}{4}$ and $|s|\le\frac{3}{2}$, each system of continuous shearlets spans a subspace of $L^2(\mathbb{R}^2)$ consisting of functions having Fourier-domain supports in one of the horizontal or vertical cones defined in the Fourier domain by

$$\mathscr{P}^{(h)} = \{(\xi_1,\xi_2) \in \mathbb{R}^2 : |\xi_1| \geq 2 \text{ and } |\tfrac{\xi_2}{\xi_1}| \leq 1\}$$
$$\mathscr{P}^{(v)} = \{(\xi_1,\xi_2) \in \mathbb{R}^2 : |\xi_1| \geq 2 \text{ and } |\tfrac{\xi_2}{\xi_1}| > 1\}.$$

The following proposition shows that the horizontal and vertical shearlets satisfy a reproducing formula similar to (10) for the spaces of L^2 functions whose Fourier-domain support is contained in $\mathscr{P}^{(h)}$ and $\mathscr{P}^{(h)}$, respectively. The proof of this result is similar to Proposition 2 and is omitted.

Proposition 3. *Let $\psi^{(h)}$ and $\psi^{(v)}$ be chosen with $\hat{\psi}_1$ and $\hat{\psi}_2$ satisfying* (9)*. Let*

$$L^2(\mathscr{P}^{(h)})^\vee = \{f \in L^2(\mathbb{R}^2) : \operatorname{supp} \hat{f} \subset \mathscr{P}^{(h)}\},$$

with a similar definition for $L^2(\mathscr{P}^{(v)})^\vee$. We have the following.

(i) For all $f \in L^2(\mathscr{P}^{(h)})^\vee$,

$$f = \int_{\mathbb{R}^2} \int_{-2}^{2} \int_{0}^{\frac{1}{4}} \langle f, \psi^{(h)}_{a,s,t} \rangle \, \psi^{(h)}_{a,s,t}(x) \, \frac{da}{a^3} \, ds \, dt.$$

(ii) For all $f \in L^2(\mathscr{P}^{(v)})^\vee$,

$$f = \int_{\mathbb{R}^2} \int_{-2}^{2} \int_{0}^{\frac{1}{4}} \langle f, \psi^{(v)}_{a,s,t} \rangle \, \psi^{(v)}_{a,s,t}(x) \, \frac{da}{a^3} \, ds \, dt.$$

The equalities are understood in the L^2 sense.

Using the horizontal and vertical shearlets, we define the *(fine-scale) continuous shearlet transform* on $L^2(\mathbb{R}^2)$ as the mapping

$$f \in L^2(\mathbb{R}^2 \setminus [-2,2]^2)^\vee \to \mathscr{SH}_\psi f(a,s,t), \quad a \in (0, \tfrac{1}{4}], s \in [-\infty,\infty], t \in \mathbb{R}^2,$$

given by

$$\mathscr{SH}_\psi f(a,s,t) = \begin{cases} \mathscr{SH}^{(h)}_\psi f(a,s,t) = \langle f, \psi^{(h)}_{a,s,t} \rangle, & \text{if } |s| \leq 1 \\ \mathscr{SH}^{(v)}_\psi f(a,\frac{1}{s},t) = \langle f, \psi^{(v)}_{a,s,t} \rangle, & \text{if } |s| > 1. \end{cases}$$

In this expression, it is understood that the limit value $s = \pm\infty$ is defined and that $\mathscr{SH}_\psi f(a,\pm\infty,t) = \mathscr{SH}^{(v)}_\psi f(a,0,t)$.

The term *fine-scale* refers to the fact that this shearlet transform is only defined for the scale variable $a \in (0,1/4]$, corresponding to "fine scales". In fact, as it is clear from Proposition 3, the shearlet transform $\mathscr{SH}_\psi f$ defines an isometry on $L^2(\mathbb{R}^2 \setminus [-2,2]^2)^\vee$, the subspace of $L^2(\mathbb{R}^2)$ of functions with Fourier-domain support away from $[-2,2]^2$, but not on $L^2(\mathbb{R}^2)$. This is not a limitation since the shearlet-based analysis of singularities we will present below is based on asymptotic estimates, as a approaches 0. In the following, for brevity, we will drop the wording 'fine-scale' and, henceforth, simply refer to this transform as the *continuous shearlet transform*.

3 Shearlet analysis of step edges. Case $n = 2$.

In this section, we show that the continuous shearlet transform provides a precise geometric characterization of step edges for functions of two variables of the form χ_S, where $S \subset \mathbb{R}^2$ is a compact set with piecewise regular boundary.

Before presenting the general result, we will examine again the two-dimensional Heaviside step function that we analyzed above using the conventional wavelet transform. The examination of this example is useful to illustrate the properties of the continuous shearlet transform. A direct calculation, where we use Plancherel theorem and denote $t = (t_1, t_2) \in \mathbb{R}^2$, yields that, for $|s| < 1$, we have

$$\begin{aligned}
\mathcal{SH}_\psi H(a,s,t) &= \langle H, \psi^{(h)}_{a,s,t} \rangle \\
&= \int_{\mathbb{R}^2} \hat{H}(\xi_1,\xi_2)\, \overline{\hat{\psi}^{(h)}_{a,s,t}}(\xi_1,\xi_2)\, d\xi_1\, d\xi_2 \\
&= \int_{\mathbb{R}^2} \frac{\delta_2(\xi_1,\xi_2)}{2\pi i \xi_1}\, \overline{\hat{\psi}^{(h)}_{a,s,t}}(\xi_1,\xi_2)\, d\xi_1\, d\xi_2 \\
&= \int_{\mathbb{R}} \frac{1}{2\pi i \xi_1}\, \overline{\hat{\psi}_{a,s,t}}(\xi_1,0)\, d\xi_1 \\
&= a^{\frac{1+\beta}{2}} \int_{\mathbb{R}} \frac{1}{2\pi i \xi_1}\, \overline{\hat{\psi}_1}(a\,\xi_1)\, \overline{\hat{\psi}_2}(a^{\beta-1}s)\, e^{2\pi i \xi_1 t_1}\, d\xi_1 \\
&= a^{\frac{1+\beta}{2}}\, \overline{\hat{\psi}_2}(a^{\beta-1}s) \int_{\mathbb{R}} \hat{\gamma}(\eta)\, e^{2\pi i \eta \frac{t_1}{a}}\, d\eta,
\end{aligned}$$

where $\hat{\gamma}(\eta) = \frac{1}{2\pi i \eta}\overline{\hat{\psi}_1}(\eta)$. Hence, using the assumption that $\hat{\psi}_1 \in C_c^\infty(\mathbb{R})$, we have that $\mathcal{SH}_\psi H(a,s,t)$ exhibits rapid asymptotic decay, as $a \to 0$, for all $(t_1,t_2) \in \mathbb{R}^2$ when $t_1 \neq 0$. If $t_1 = 0$ and $s \neq 0$, the term $\overline{\hat{\psi}_2}(a^{\beta-1}s)$ will vanish as $a \to 0$, due to the support assumptions on $\hat{\psi}_2$. Finally, if $t_1 = 0$ and $s = 0$, we have that

$$\mathcal{SH}_\psi H(a,0,(0,t_2)) = a^{\frac{1+\beta}{2}}\, \overline{\hat{\psi}_2}(0) \int_{\mathbb{R}} \hat{\gamma}(\eta)\, d\eta.$$

Hence, provided that $\hat{\psi}_2(0) \neq 0$ and $\int_{\mathbb{R}} \hat{\gamma}(\eta)\, d\eta \neq 0$, we have the estimate

$$\mathcal{SH}_\psi H(a,0,(0,t_2)) = O(a^{\frac{1+\beta}{2}}).$$

A similar computation shows that $\mathcal{SH}_\psi H(a,s,t)$ exhibits rapid asymptotic decay, as $a \to 0$, for all $|s| > 1$.

In summary, under appropriate assumptions on ψ_1 and ψ_2, we observe that *the continuous shearlet transform of H decays rapidly, asymptotically for $a \to 0$, for all t and s, unless t is on the discontinuous line and s corresponds to the normal direction of the discontinuous line at t. Thus, with respect to the wavelet-based analysis, the shearlet-based approach enables to detect both the location and orientation of the discontinuous line.*

Remarkably, the same properties of the continuous shearlet transform observed on the two-dimensional Heaviside step function can be extended to very general functions containing step discontinuities.

In particular, let us consider $f = \chi_S$ where $S \subset \mathbb{R}^2$ is a compact region whose boundary, denoted by ∂S, is a simple curve, of finite length L, smooth except possibly for finitely many corner points. To define the notion of corner point, let $\alpha(t)$ be the parametrization of ∂S with respect to the arc length parameter t. For any $t_0 \in (0,L)$ and any $j \geq 0$, we assume that $\lim_{t\to t_0^-} \alpha^{(j)}(t) = \alpha^{(j)}(t_0^-)$ and $\lim_{t\to t_0^+} \alpha^{(j)}(t) = \alpha^{(j)}(t_0^+)$ exist. Also, let $\mathbf{n}(t^-)$, $\mathbf{n}(t^+)$ be the outer normal direction(s) of ∂S at $\alpha(t)$ from the left and right, respectively; if they are equal, we write them as $\mathbf{n}(t)$. Similarly, for the curvature of ∂S, we use the notation $\kappa(t^-)$, $\kappa(t^+)$ and $\kappa(t)$. We say that $p = \alpha(t_0)$ is a *corner point of* ∂S if either (i) $\alpha'(t_0^-) \neq \pm\alpha'(t_0^+)$ or (ii) $\alpha'(t_0^-) = \pm\alpha'(t_0^+)$, but $\kappa(t_0^-) \neq \kappa(t_0^+)$. When (i) holds, we say that p is a *corner point of first type* and, when (ii) holds, we say that p is a *corner point of second type*. On the other hand, if $\alpha(t)$ is infinitely many times differentiable at t_0, we say that $\alpha(t_0)$ is a *regular point* of ∂S. The boundary curve $\alpha(t)$ is *piecewise smooth* if the values $\alpha(t)$ are regular points for all $0 \leq t \leq L$, except for finitely many corner points. Note that it is not necessary to require infinite regularity. One can replace the piecewise smooth boundary with a piecewise regular boundary of finite order, say C^m (for sufficiently large m), and derive a result similar to the one we will discuss below, at the cost of heavier notation.

Let $p_0 = \alpha(t_0)$ be a regular point and let $s_0 = \tan(\theta_0)$ with $\theta_0 \in (-\frac{\pi}{2}, \frac{\pi}{2})$. Let $\Theta(\theta_0) = [\cos\theta_0, \sin\theta_0]$. We say that s_0 *corresponds to the normal direction of* ∂S *at* p_0 if $\Theta(\theta_0) = \pm\mathbf{n}(t_0)$. When $\alpha(t_0)$ is a corner point, we can identify two outer normal directions $\mathbf{n}(t_0^-)$ and $\mathbf{n}(t_0^+)$.

We are now ready to state the following results which is a generalization of a similar result originally proved in [19] for the special case $\beta = 1/2$.

Theorem 1. *Let* ψ_1, ψ_2 *be chosen such that*

- $\hat{\psi}_1 \in C_c^\infty(\mathbb{R})$, $\operatorname{supp}\hat{\psi}_1 \subset [-2,-\frac{1}{2}] \cup [\frac{1}{2},2]$, *is odd, nonnegative on* $[\frac{1}{2},2]$ *and it satisfies* $\displaystyle\int_0^\infty |\hat{\psi}_1(a\xi)|^2 \frac{da}{a} = 1$, *for a.e.* $\xi \in \mathbb{R}$;
- $\hat{\psi}_2 \in C_c^\infty(\mathbb{R})$, $\operatorname{supp}\hat{\psi}_2 \subset [-\frac{\sqrt{2}}{4}, \frac{\sqrt{2}}{4}]$, *is even, nonnegative, decreasing in* $[0, \frac{\sqrt{2}}{4})$, *and* $\|\psi_2\|_2 = 1$.

Let $B = \chi_S$, *where* $S \subset \mathbb{R}^2$ *is a compact set whose boundary* ∂S *is piecewise smooth, and let* $k(p)$ *be the curvature of* ∂S *at the point* p. *The following estimates hold.*

(i) If $p \notin \partial S$ *then, for all* $s \in \mathbb{R}$,

$$\lim_{a\to 0^+} a^{-N}\, \mathscr{SH}_\psi B(a,s,p) = 0, \quad \text{for all } N > 0.$$

(ii) If $p_0 \in \partial S$ *is a regular point,* s_0 *corresponds to the normal direction of* ∂S *at* p_0 *and* $s \neq s_0$, *then*

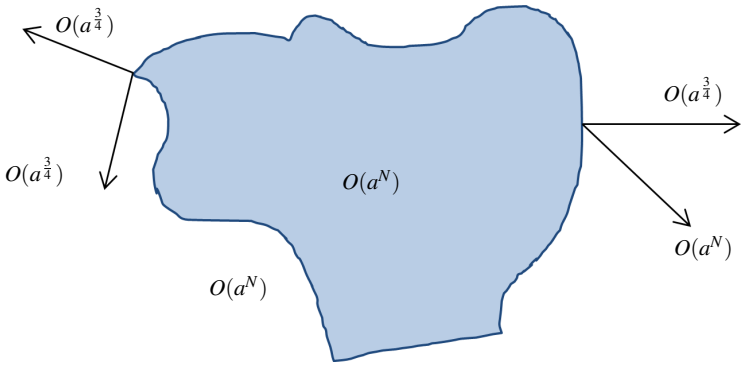

Fig. 2 Asymptotic decay rate of the continuous shearlet transform of $B = \chi_S$, where $S \subset \mathbb{R}^2$ has piecewise smooth boundary. Here we consider the case where $\beta = \frac{1}{2}$. Away from the boundary, the decay is faster than $O(a^N)$, for any $N \in \mathbb{N}$. At the regular points $p \in \partial S$, for s corresponding to the normal orientation, the shearlet transform decays as $O(a^{\frac{3}{4}})$; for all other values of s, the decay is faster than $O(a^N)$, for any $N \in \mathbb{N}$. At a corner point p, the shearlet transform decays as $O(a^{\frac{3}{4}})$ for the values of s associated with the two normal orientations at p.

$$\lim_{a\to 0^+} a^{-N} \mathcal{SH}_\psi B(a,s,p_0) = 0, \quad \textit{for all } N > 0.$$

(iii) If $p_0 \in \partial S$ is a regular point, s_0 corresponds to the normal direction of ∂S at p_0, $k(p_0) = 0$, and $\frac{1}{3} < \beta < 1$, then

$$\lim_{a\to 0^+} a^{-\frac{1+\beta}{2}} \mathcal{SH}_\psi B(a,s_0,p_0) \neq 0.$$

(iv) If $p_0 \in \partial S$ is a regular point, s_0 corresponds to the normal direction of ∂S at p_0, $k(p_0) \neq 0$, and $0 < \beta \leq \frac{1}{2}$, then

$$\lim_{a\to 0^+} a^{-(1-\frac{\beta}{2})} \mathcal{SH}_\psi B(a,s_0,p_0) \neq 0.$$

(v) If $p_0 \in \partial S$ is a regular point, s_0 corresponds to the normal direction of ∂S at p_0, $k(p_0) \neq 0$, and $\frac{1}{2} \leq \beta < 1$, then

$$\lim_{a\to 0^+} a^{-\frac{1+\beta}{2}} \mathcal{SH}_\psi B(a,s_0,p_0) \neq 0.$$

Remark 1. The theorem shows that, when $p \notin \partial S$ or when $p \in \partial S$ but s does not correspond to the normal direction of ∂S at p, then the continuous shearlet transform $\mathcal{SH}_\psi B(a,s,p)$ exhibits rapid asymptotic decay, as a function of a, when a approached 0. If $p \in \partial S$ is a regular point and s corresponds to the normal direction of ∂S at p, then the continuous shearlet transform has 'slow' asymptotic decay, with

decay rate depending on the curvature k of ∂S at p. In particular, when $\frac{1}{3} < \beta < \frac{1}{2}$, the decay rates are $O(a^{\frac{1+\beta}{2}})$ and $O(a^{(1-\frac{\beta}{2})})$ when $k(p) = 0$ and $k(p) \neq 0$, respectively. When $\beta = \frac{1}{2}$, the theorem recovers the results from [19], where the decay rate is $O(a^{\frac{3}{4}})$, independently of the values of $k(p)$.

In the case where $p \in \partial S$ is a corner point, the shearlet analysis also provides a precise characterization. We recall below the following result from [19], valid when $\beta = \frac{1}{2}$. The result for general β is not known at this time.

Theorem 2. *Let ψ_1, ψ_2 be chosen as in Theorem 1 and $\beta = \frac{1}{2}$. For $B = \chi_S$, where $S \subset \mathbb{R}^2$ is a compact set whose boundary ∂S is piecewise smooth, the following holds.*

(i) If $p_0 \in \partial S$ is a corner point of the first type and s does not correspond to any of the normal directions of ∂S at p_0, then

$$\lim_{a \to 0^+} a^{-\frac{9}{4}} \mathcal{SH}_\psi B(a, s, p_0) < \infty.$$

(ii) If $p_0 \in \partial S$ is a corner point of the second type and s does not correspond to any of the normal directions of ∂S at p_0, then

$$\lim_{a \to 0^+} a^{-\frac{9}{4}} \mathcal{SH}_\psi B(a, s, p_0) \neq 0.$$

(iii) If $p_0 \in \partial S$ is a corner point and $s = s_0$ corresponds to one of the normal directions of ∂S at p_0 then

$$\lim_{a \to 0^+} a^{-\frac{3}{4}} \mathcal{SH}_\psi B(a, s_0, p_0) \neq 0.$$

That is, at a corner points p_0, the asymptotic decay of the continuous shearlet transform depends both on the tangent and the curvature at p_0. If $s = s_0$ corresponds to one of the normal directions of ∂S at p_0, then the continuous shearlet transform decays as

$$\mathcal{SH}_\psi B(a, s_0, p_0) \sim O(a^{\frac{3}{4}}), \text{ as } a \to 0,$$

similar to the situation of regular boundary points. If p_0 is a corner point of the second type (e.g., the corner point in a half-disk) and s does not correspond to any of the normal directions, then

$$\mathcal{SH}_\psi B(a, s, p_0) \sim O(a^{\frac{9}{4}}), \text{ as } a \to 0,$$

which is a faster decay rate than in the normal-orientation case. Finally, if p_0 is a corner point of the first type (e.g., the vertex of a polygon) and s does not correspond to any of the normal directions, then, by the theorem, we only know that the asymptotic decay of $|\mathcal{SH}_\psi B(a, s_0, p)|$ is not slower than $O(a^{\frac{9}{4}})$. However the decay could be faster than $O(a^{\frac{9}{4}})$, as shown in [19].

The asymptotic decay rate of the continuous shearlet transform $\mathcal{SH}_\psi B(a,s,p)$, as $a \to 0$, for various values of s and p is illustrated in Fig. 5.

3.1 Proof of Theorem 1

It is clear that the argument used to estimate the continuous shearlet transform of the two-dimensional Heaviside step function cannot be extended to this case directly since this would require an explicit expression of the Fourier transform of the function $B = \chi_S$. In this more general case, we will instead apply the divergence theorem. This theorem allows us to express the Fourier transform of B as a line integral over ∂S:

$$\begin{aligned}\hat{B}(\xi) = \widehat{\chi}_S(\xi) &= -\frac{1}{2\pi i|\xi|}\int_{\partial S} e^{-2\pi i \xi\cdot x}\,\Theta(\theta)\cdot\mathbf{n}(x)\,d\sigma(x)\\ &= -\frac{1}{2\pi i\rho}\int_0^L e^{-2\pi i\rho\,\Theta(\theta)\cdot\alpha(t)}\,\Theta(\theta)\cdot\mathbf{n}(t)\,dt \qquad (12)\end{aligned}$$

where $\xi = \rho\,\Theta(\theta)$, $\Theta(\theta) = (\cos\theta, \sin\theta)$. Note that this convenient idea for representing the Fourier transform of the characteristic function of a bounded region is used, for example, in [26].

Hence, using (12), we have that

$$\begin{aligned}&\mathcal{SH}_\psi B(a,s,p)\\ &= \langle B, \psi_{a,s,p}\rangle\\ &= \int_0^{2\pi}\int_0^{\infty} \hat{B}(\rho,\theta)\,\overline{\hat{\psi}^{(d)}_{a,s,p}}(\rho,\theta)\,\rho\,d\rho\,d\theta\\ &= -\frac{1}{2\pi i}\int_0^{2\pi}\int_0^{\infty}\int_0^{L}\overline{\hat{\psi}^{(d)}_{a,s,p}}(\rho,\theta)e^{-2\pi i\rho\,\Theta(\theta)\cdot\alpha(t)}\,\Theta(\theta)\cdot\mathbf{n}(t)\,dt\,d\rho\,d\theta, \qquad (13)\end{aligned}$$

where the upper-script in $\psi^{(d)}_{a,s,p}$ is either $d = h$, when $|s| \le 1$, or $d = v$, when $|s| > 1$.

The first simplifying observation is that the asymptotic decay of the shearlet transform $\mathcal{SH}_\psi B(a,s,p)$, as $a \to 0$, is only determined by the values of the boundary ∂S which are "close" to p. To state this fact, for $\varepsilon > 0$, let $D(\varepsilon,p)$ be the ball in $\mathbb{R}^2$ of radius ε and center p, and $D^c(\varepsilon,p) = \mathbb{R}^2 \setminus D(\varepsilon,p)$. Hence, using (13), we can write the shearlet transform of B as

$$\mathcal{SH}_\psi B(a,s,p) = I_1(a,s,p) + I_2(a,s,p),$$

where

$$I_1(a,s,p) = -\frac{1}{2\pi i}\int_0^{2\pi}\int_0^{\infty}\int_{\partial S\cap D(\varepsilon,p)} \overline{\hat{\psi}^{(d)}_{a,s,p}}(\rho,\theta)e^{-2\pi i\rho\,\Theta(\theta)\cdot\alpha(t)}\Theta(\theta)\cdot\mathbf{n}(t)\,dt\,d\rho\,d\theta, \quad (14)$$

$$I_2(a,s,p) = -\frac{1}{2\pi i}\int_0^{2\pi}\int_0^{\infty}\int_{\partial S\cap D^c(\varepsilon,p)} \overline{\hat{\psi}^{(d)}_{a,s,p}}(\rho,\theta)e^{-2\pi i\rho\,\Theta(\theta)\cdot\alpha(t)}\Theta(\theta)\cdot\mathbf{n}(t)\,dt\,d\rho\,d\theta. \quad (15)$$

The following Localization Lemma shows that I_2 has rapid asymptotic decay, at fine scales.

Lemma 1 (Localization Lemma). *Let $I_2(a,s,p)$ be given by (15). For any positive integer N, there is a constant $C_N > 0$ such that*

$$|I_2(a,s,p)| \le C_N\, a^{\frac{N}{2}},$$

asymptotically as $a \to 0$, uniformly for all $s \in \mathbb{R}$.

Proof. We will only examine the behaviour of $I_2(a,s,p)$ for $|s| \le 1$, so that we use the horizontal shearlets only. The proof when $|s| > 1$ is similar. We have:

$$\begin{aligned}
I_2(a,s,p) &= -\frac{1}{2\pi i}\int_{\partial S\cap D^c(\varepsilon,p)}\int_0^{2\pi}\int_0^{\infty} \overline{\hat{\psi}^{(h)}_{a,s,p}}(\rho,\theta)e^{-2\pi i\rho\,\Theta(\theta)\cdot\alpha(t)}\,\Theta(\theta)\cdot\mathbf{n}(t)\,dt\,d\rho\,d\theta \\
&= \frac{-a^{\frac{1+\beta}{2}}}{2\pi i}\int_{\partial S\cap D^c(\varepsilon,p)}\int_0^{2\pi}\int_0^{\infty} \hat{\psi}_1(a\rho\,\cos\theta)\,\hat{\psi}_2(a^{\beta-1}(\tan\theta - s)) \\
&\quad \times e^{2\pi i\rho\,\Theta(\theta)\cdot p}\,d\rho\,d\theta e^{-2\pi i\rho\,\Theta(\theta)\cdot\alpha(t)}\,\Theta(\theta)\cdot\mathbf{n}(t)\,dt \\
&= \frac{-a^{\frac{\beta-1}{2}}}{2\pi i}\int_{\partial S\cap D^c(\varepsilon,p)}\int_0^{2\pi}\int_0^{\infty} \hat{\psi}_1(\rho\,\cos\theta)\,\hat{\psi}_2(a^{\beta-1}(\tan\theta - s)) \\
&\quad \times e^{2\pi i\frac{\rho}{a}\,\Theta(\theta)\cdot(p-\alpha(t))}\,\Theta(\theta)\cdot\mathbf{n}(t)\,d\rho\,d\theta\,dt.
\end{aligned}$$

By assumption, since integration occurs on the region $D^c(\varepsilon,p)$, we have that $\|p-\alpha(t)\| \ge \varepsilon$ for all $\alpha(t) \in \partial S\cap D^c(\varepsilon,p)$. Hence, there is a constant C_p such that $\inf_{x\in\partial S\cap D^c(\varepsilon,p)}|p-x| = C_p$. Note that, due to the assumptions on the support on $\hat{\psi}_2$, the integration in the variable θ is restricted to the interval $\mathscr{I} = \{\theta : |\tan\theta - s| \le a^{1-\beta}\}$. Let $\mathscr{I}_1 = \{\theta : |\Theta(\theta)\cdot(p-x)| \ge \frac{C_p}{\sqrt{2}}\}\bigcap\mathscr{I}$, and $\mathscr{I}_2 = \mathscr{I}\setminus\mathscr{I}_1$. Since the vectors $\Theta(\theta), \Theta'(\theta)$ form an orthonormal basis in $\mathbb{R}^2$, it follows that, on the set $\mathscr{I}_2$, we have $|\Theta'(\theta)\cdot(p-x)| \ge \frac{C_p}{\sqrt{2}}$. Hence we can express the integrals I_2 as a sum of a term where $\theta \in \mathscr{I}_1$ and another term where $\theta \in \mathscr{I}_2$, and integrate by parts as follows. On $\mathscr{I}_1$, we integrate by parts with respect to the variable ρ; on $\mathscr{I}_2$ we integrate by parts with respect to the variable θ. Doing this repeatedly, it yields that, for any positive integer N, $|I_2(a,s,p)| \le C_N\, a^{\beta N}$, uniformly in s. This finishes the proof of the lemma. □

Let $\alpha(t)$ be the boundary curve ∂S, with $0 \le t \le L$ and $p \in \partial S$. Without loss of generality we may assume that $L > 1$ and $p = (0,0) = \alpha(1)$. If p is a regular point,

we write the boundary curve near p as $\mathscr{C} = \partial S \cap D(\varepsilon,(0,0))$, where

$$\mathscr{C} = \{\alpha(t) : 1-\varepsilon \le t \le 1+\varepsilon\}.$$

Rather than using the arclength representation of $\mathscr{C}$, we can also write $\mathscr{C} = \{(G(u),u),\, -\varepsilon \le u \le \varepsilon\}$, where $G(u)$ is a smooth function. Since $p=(0,0)$, we have $G(0)=0$.

If p is a corner point of ∂S, we write the boundary curve near p as $\mathscr{C} = \partial S \cap D(\varepsilon,(0,0)) = \mathscr{C}^- \cup \mathscr{C}^+$, where

$$\mathscr{C}^- = \{\alpha(t) : 1-\varepsilon \le t \le 1\}, \quad \mathscr{C}^+ = \{\alpha(t) : 1 \le t \le 1+\varepsilon\}.$$

Similar to the regular point case, we can write $\mathscr{C}^+ = \{(G^+(u),u),\, 0 \le u \le \varepsilon\}$ and $\mathscr{C}^- = \{(G^-(u),u),\, -\varepsilon \le u \le 0\}$, where $G^+(u)$ and $G^-(u)$ are smooth functions on $[0,\varepsilon]$ and $[-\varepsilon,0]$, respectively.

We will need the following Lemma which is proven in [19].

Lemma 2. *Let $\psi_2 \in L^2(\mathbb{R})$ be such that $\|\psi_2\|_2 = 1$, $\operatorname{supp}\hat{\psi}_2 \subset [-1,1]$, $\hat{\psi}_2$ is even, nonnegative and decreasing on $[0,1]$. Then, for each $\rho > 0$, we have that*

$$\int_0^1 \hat{\psi}_2(u)\left(\sin(\pi\rho u^2)+\cos(\pi\rho u^2)\right) du > 0.$$

We can now proceed with the proof of Theorem 1.

Proof of Theorem 1.

As above, it will be sufficient to examine the case of the horizontal shearlets only; the case of vertical shearlets is similar.

• *Part (i)* This follows directly from Lemma 1.

• *Part (ii)* Assume that $s = s_0$ does not correspond to any of the normal directions of ∂S at $p=(0,0)$. We write $s_0 = \tan\theta_0$, where we assume that $|\theta_0| \le \frac{\pi}{4}$. Otherwise, for the case $\frac{\pi}{4} < |\theta_0| \le \frac{\pi}{2}$, one will use the vertical shearlets and the argument is very similar to the one presented below. Hence, we have that

$$I_1(a,s_0,0) = -\frac{a^{\frac{\beta-1}{2}}}{2\pi i}\int_0^\infty\int_0^{2\pi} \hat{\psi}_1(\rho\cos\theta)\,\hat{\psi}_2(a^{\beta-1}(\tan\theta-\tan\theta_0))K(a,\rho,\theta)\,d\theta\,d\rho,$$

where

$$K(a,\rho,\theta) = \int_{1-\varepsilon}^{1+\varepsilon} e^{-2\pi i\frac{\rho}{a}\Theta(\theta)\cdot\alpha(t)}\,\Theta(\theta)\cdot\mathbf{n}(t)\,dt.$$

Let $b \in C_0^\infty(\mathbb{R})$ be a smooth bump function such that $b(t)=1$ for $|t-1| \le \frac{\varepsilon}{4}$ and $b(t)=0$ for $|t-1| > \frac{3\varepsilon}{4}$. Hence we can write

$$I_1(a,s_0,0) = I_{11}(a,s_0,0) + I_{12}(a,s_0,0),$$

where

$$I_{11}(a,s_0,0) = -\frac{a^{\frac{\beta-1}{2}}}{2\pi i}\int_0^\infty\int_0^{2\pi} \hat{\psi}_1(\rho\cos\theta)\,\hat{\psi}_2(a^{\beta-1}(\tan\theta-\tan\theta_0))K_1(a,\rho,\theta)\,d\theta\,d\rho,$$

$$I_{12}(a,s_0,0) = -\frac{a^{\frac{\beta-1}{2}}}{2\pi i}\int_0^\infty\int_0^{2\pi} \hat{\psi}_1(\rho\cos\theta)\,\hat{\psi}_2(a^{\beta-1}(\tan\theta-\tan\theta_0))K_2(a,\rho,\theta)\,d\theta\,d\rho,$$

and

$$K_1(a,\rho,\theta) = \int_{1-\varepsilon}^{1+\varepsilon} e^{-2\pi i\frac{\rho}{a}\Theta(\theta)\cdot\alpha(t)}\,\Theta(\theta)\cdot\mathbf{n}(t)\,b(t)\,dt$$

$$K_2(a,\rho,\theta) = \int_{1-\varepsilon}^{1+\varepsilon} e^{-2\pi i\frac{\rho}{a}\Theta(\theta)\cdot\alpha(t)}\,\Theta(\theta)\cdot\mathbf{n}(t)\,(1-b(t))\,dt.$$

From the definition of $b(t)$, we have $1-b(t)=0$ for $|t-1|\le\frac{\varepsilon}{4}$. Since the boundary curve $\{\alpha(t),\,0\le t\le L\}$ is simple and $p=(0,0)=\alpha(1)$, it follows that there exists a $c_0>0$ such that $\|\alpha(t)\|\ge c_0$ for all t with $\frac{\varepsilon}{4}\le|t-1|\le\varepsilon$. Replacing the set $D^c(\varepsilon,p)$ by the set $\{\alpha(t),\,\frac{\varepsilon}{4}\le|t-1|\le\varepsilon\}$, one can repeat the argument of Lemma 1 for $I_{12}(a,s_0,0)$ to show that $|I_{12}(a,s_0,0)|\le C_N a^N$ for any $N>0$.

Recall that when $a\to 0$, we have $\theta\to\theta_0$. Since s_0 does not correspond to the normal direction at p, one can choose ε sufficient small so that $\Theta(\theta)\cdot\alpha'(t)\neq 0$ for $|t-1|\le\varepsilon$ and for all small a (and hence for θ near θ_0). Also from the assumption on b, it follows that $b^{(n)}(1-\varepsilon)=0$ and $b^{(n)}(1+\varepsilon)=0$ for all $n\ge 0$. Writing

$$e^{-2\pi i\frac{\rho}{a}\Theta(\theta)\cdot\alpha(t)} = \frac{-a}{2\pi i\rho\,\Theta(\theta)\cdot\alpha'(t)}\left(e^{-2\pi i\frac{\rho}{a}\Theta(\theta)\cdot\alpha(t)}\right)',$$

it follows that

$$\begin{aligned}
K_1(a,\rho,\theta) &= -\frac{a}{2\pi i\rho}\int_{1-\varepsilon}^{1+\varepsilon}\left(e^{-2\pi i\frac{\rho}{a}\Theta(\theta)\cdot\alpha(t)}\right)'\frac{\Theta(\theta)\cdot\mathbf{n}(t)}{\Theta(\theta)\cdot\alpha'(t)}\,b(t)\,dt\\
&= \frac{ai}{2\pi\rho}\left(\left(e^{-2\pi i\frac{\rho}{a}\Theta(\theta)\cdot\alpha(t)}\frac{\Theta(\theta)\cdot\mathbf{n}(t)}{\Theta(\theta)\cdot\alpha'(t)}\,b(t)\right)_{1-\varepsilon}^{1+\varepsilon}+K_3(a,\rho,\theta)\right)\\
&= \frac{ai}{2\pi\rho}K_3(a,\rho,\theta),
\end{aligned}$$

where we used the fact that $b(1-\varepsilon)=0$, $b(1+\varepsilon)=0$ and

$$K_3(a,\rho,\theta) = \int_{1-\varepsilon}^{1+\varepsilon} e^{-2\pi i\frac{\rho}{a}\Theta(\theta)\cdot\alpha(t)}\left(\frac{\Theta(\theta)\cdot\mathbf{n}(t)}{\Theta(\theta)\cdot\alpha'(t)}\,b(t)\right)'dt.$$

Repeating the above argument for $K_3(a,\rho,\theta)$ and using induction, it follows that for all $N>0$ there exists a $C_N>0$ such that $|K_1(a,\rho,\theta)|\le C_N a^N$ and, hence, that $|I_{11}(a,s_0,0)|\le C_N a^N$.

• *Part (iii)* Without loss of generality, we may assume that $p = (0,0)$ and $s_0 = 0$ so that $\tan\theta_0 = 0$ (and hence $G'(0) = 0$). It follows that $G(u) = Au^2 + O(u^3)$ near $u = 0$ with some constant A. Since $G''(0) = 0$ by assumption in this case, we have $A = 0$.

Using polar coordinates, we can express $I_1(a,0,0)$, evaluated on $s_0 = 0$, as

$$\begin{aligned} &I_1(a,0,0) \\ &= -\frac{a^{\frac{\beta-1}{2}}}{2\pi i}\int_0^\infty\int_0^{2\pi}\hat\psi_1(\rho\cos\theta)\hat\psi_2(a^{1-\beta}\tan\theta)\int_{-\varepsilon}^{\varepsilon} e^{-2\pi i\frac{\rho}{a}(\cos\theta O(u^3)+\sin\theta\, u)} \\ &\times(-\cos\theta+\sin\theta\, O(u^2))\,du\,d\theta\,d\rho. \end{aligned}$$

By Lemma 1, to complete the proof of this case it is sufficient to show that

$$\lim_{a\to 0^+} a^{-\frac{1+\beta}{2}} I_1(a,s_0,0) \neq 0.$$

In the expression of I_1, the interval $[0,2\pi]$ of the integral in θ can be broken into the subintervals $[-\frac{\pi}{2},\frac{\pi}{2}]$ and $[\frac{\pi}{2},\frac{3\pi}{2}]$. On $[\frac{\pi}{2},\frac{3\pi}{2}]$, we let $\theta' = \theta - \pi$ so that $\theta' \in [-\frac{\pi}{2},\frac{\pi}{2}]$ and $\sin\theta = -\sin\theta'$, $\cos\theta = -\cos\theta'$. Using this observation and the fact that $\hat\psi_1$ is an odd function, it follows that $I_1(a,0,0) = I_{10}(a,0,0) + I_{11}(a,0,0)$, where

$$\begin{aligned} &2\pi i\, a^{\frac{1-\beta}{2}} I_{10}(a,0,0) \\ &= \cos\theta\int_0^\infty\int_{-\frac{\pi}{2}}^{\frac{\pi}{2}}\hat\psi_1(\rho\cos\theta)\hat\psi_2(a^{1-\beta}\tan\theta)\int_{-\varepsilon}^{\varepsilon} e^{-2\pi i\frac{\rho}{a}(\cos\theta O(u^3)+u\sin\theta)}du\,d\theta\,d\rho \\ &+\cos\theta\int_0^\infty\int_{-\frac{\pi}{2}}^{\frac{\pi}{2}}\hat\psi_1(\rho\cos\theta)\hat\psi_2(a^{1-\beta}\tan\theta)\int_{-\varepsilon}^{\varepsilon} e^{2\pi i\frac{\rho}{a}(\cos\theta O(u^3)+u\sin\theta)}\,du\,d\theta\,d\rho, \end{aligned}$$

and

$$\begin{aligned} &2\pi i\, a^{\frac{1-\beta}{2}} I_{11}(a,0,0) \\ &= -\sin\theta\int_0^\infty\int_{-\frac{\pi}{2}}^{\frac{\pi}{2}}\hat\psi_1(\rho\cos\theta)\hat\psi_2(a^{1-\beta}\tan\theta)\int_{-\varepsilon}^{\varepsilon} e^{-2\pi i\frac{\rho}{a}(\cos\theta O(u^3)+u\sin\theta)}O(u^2)du\,d\theta\,d\rho \\ &-\sin\theta\int_0^\infty\int_{-\frac{\pi}{2}}^{\frac{\pi}{2}}\hat\psi_1(\rho\cos\theta)\hat\psi_2(a^{1-\beta}\tan\theta)\int_{-\varepsilon}^{\varepsilon} e^{2\pi i\frac{\rho}{a}(\cos\theta O(u^3)+u\sin\theta)}O(u^2)\,du\,d\theta\,d\rho. \end{aligned}$$

For $\theta \in (-\frac{\pi}{2},\frac{\pi}{2})$, let $t = a^{\beta-1}\tan\theta$ and $u = a^\beta v$. We observe that $a \to 0$ implies $\theta \to 0$. It is easy to see that $\lim_{a\to 0}\frac{1}{a}(\sin\theta u) = \lim_{a\to 0}\frac{1}{a}(\cos\theta a^{1-\beta+\beta}tv) = tv$ and that, for $\frac{1}{3} < \beta < 1$, we have $\lim_{a\to 0}\frac{O(u^3)}{a} = \lim_{a\to 0} a^{3\beta-1}O(v^3) = 0$.

It follows that

$$\begin{aligned}
&\lim_{a\to 0^+} 2\pi i a^{-\frac{1+\beta}{2}} I_{10}(a,0,0)\\
&= \int_0^\infty \hat{\psi}_1(\rho)\int_{-\infty}^{\infty}\int_{-1}^{1}\hat{\psi}_2(t)e^{-2\pi i\rho vt}dtdvd\rho + \int_0^\infty \hat{\psi}_1(\rho)\int_{-\infty}^{\infty}\int_{-1}^{1}\hat{\psi}_2(t)e^{2\pi i\rho vt}dtdvd\rho\\
&= 2\hat{\psi}_2(0)\int_0^\infty \hat{\psi}_1(\rho)d\rho > 0.
\end{aligned}$$

Since there is a factor $O(u^2)$ in the expression of I_{11}, the same calculation yields that $\lim_{a\to 0^+} 2\pi i a^{-\frac{1+\beta}{2}} I_{11}(a,0,0) = 0$. Through these calculations, we have hence shown that $\lim_{a\to 0^+} 2\pi i a^{-\frac{1+\beta}{2}} I_1(a,s_0,0) \neq 0$. This completes the proof of part (iii).

• *Part (iv)* We first consider the case of $\beta = \frac{1}{2}$. Since $k(p_0) \neq 0$, by assumption we have that $G(u) = Au^2 + O(u^3)$ with $A \neq 0$. Without loss of generality, we may assume $A = 1$ so that we can write $G(u) = u^2 + O(u^3)$. As in (iii), using polar coordinates, we can express $I_1(a,0,0)$, evaluated on $s_0 = 0$, as $I_1(a,0,0) = I_{10}(a,0,0) + I_{11}(a,0,0)$, where

$$\begin{aligned}
&2\pi i a^{\frac{1}{4}} I_{10}(a,0,0)\\
&= \cos\theta \int_0^\infty \int_{-\frac{\pi}{2}}^{\frac{\pi}{2}} \hat{\psi}_1(\rho\cos\theta)\hat{\psi}_2(a^{-\frac{1}{4}}\tan\theta)\int_{-\varepsilon}^{\varepsilon} e^{-2\pi i\frac{\rho}{a}(\cos\theta(u^2+O(u^3))+u\sin\theta)}du\,d\theta\,d\rho\\
&+\cos\theta \int_0^\infty \int_{-\frac{\pi}{2}}^{\frac{\pi}{2}} \hat{\psi}_1(\rho\cos\theta)\hat{\psi}_2(a^{-\frac{1}{2}}\tan\theta)\int_{-\varepsilon}^{\varepsilon} e^{2\pi i\frac{\rho}{a}(\cos\theta(u^2+O(u^3))+u\sin\theta)}du\,d\theta\,d\rho
\end{aligned}$$

and

$$\begin{aligned}
&2\pi i a^{\frac{1}{4}} I_{11}(a,0,0)\\
&= -\sin\theta \int_0^\infty \int_{-\frac{\pi}{2}}^{\frac{\pi}{2}} \hat{\psi}_1(\rho\cos\theta)\hat{\psi}_2(a^{-\frac{1}{2}}\tan\theta)\int_{-\varepsilon}^{\varepsilon} e^{-2\pi i\frac{\rho}{a}(\cos\theta(u^2+O(u^3))+u\sin\theta)}\\
&\quad\times(2u+O(u^2))du\,d\theta\,d\rho - \sin\theta\int_0^\infty\int_{-\frac{\pi}{2}}^{\frac{\pi}{2}}\hat{\psi}_1(\rho\cos\theta)\hat{\psi}_2(a^{-\frac{1}{2}}\tan\theta)\\
&\quad\times\int_{-\varepsilon}^{\varepsilon} e^{2\pi i\frac{\rho}{a}(\cos\theta(u^2+O(u^3))+u\sin\theta)}(2u+O(u^2))\,du\,d\theta\,d\rho.
\end{aligned}$$

As in part (iii), it is enough to show

$$\lim_{a\to 0^+} a^{-\frac{3}{4}} I_{10}(a,0,0) \neq 0.$$

For $\theta \in (-\frac{\pi}{2},\frac{\pi}{2})$, let $t = a^{-\frac{1}{2}}\tan\theta$ and $u = a^{-\frac{1}{2}}v$. In the calculation below, we will use the formulas of Fresnel integrals

$$\int_{-\infty}^{\infty}\cos(\frac{\pi}{2}x^2)dx = \int_{-\infty}^{\infty}\sin(\frac{\pi}{2}x^2)dx = 1.$$

Hence we have:

$$\begin{aligned}
&\lim_{a\to 0^+} 2\pi i a^{-\frac{3}{4}} I_{10}(a,0,0)\\
&= \int_0^\infty \hat{\psi_1}(\rho) \int_{-1}^1 \hat{\psi}_2(t) \int_{-\infty}^\infty e^{-2\pi i\rho(v^2+vt)}\, dv\, dt\, d\rho\\
&\quad + \int_0^\infty \hat{\psi_1}(\rho) \int_{-1}^1 \hat{\psi}_2(t) \int_{-\infty}^\infty e^{2\pi i\rho(v^2+vt)}\, dv\, dt\, d\rho\\
&= \int_0^\infty \hat{\psi_1}(\rho) \int_{-1}^1 e^{-\frac{1}{2}\pi i\rho t^2} \hat{\psi}_2(t) \int_{-\infty}^\infty e^{-2\pi i\rho(v+\frac{1}{2}t)^2}\, dv\, dt\, d\rho\\
&\quad + \int_0^\infty \hat{\psi_1}(\rho) \int_{-1}^1 e^{\frac{1}{2}\pi i\rho t^2} \hat{\psi}_2(t) \int_{-\infty}^\infty e^{2\pi i\rho(v+\frac{1}{2}t)^2}\, dv\, dt\, d\rho\\
&= \int_0^\infty \frac{\hat{\psi}_1(\rho)}{\sqrt{\rho}} \left(\int_{-1}^1 \cos(\frac{\pi\rho}{2}t^2)\hat{\psi}_2(t)\, dt + \int_{-1}^1 \sin(\frac{\pi\rho}{2}t^2)\hat{\psi}_2(t) dt \right) d\rho,
\end{aligned}$$

The last expression is strictly positive by Lemma 2 and the properties of $\hat{\psi}_1$. This completes the proof of part (iv) for $\beta = \frac{1}{2}$. It remains to prove part (iv) for $0 < \beta < \frac{1}{2}$.

We will follow the same idea as the argument for $\beta = \frac{1}{2}$ and use the change of variables $t = a^{\beta-1}\tan\theta$ and $u = \frac{1}{2}v$ (instead of $u = a^\beta v$ in the proof of part (iii)). Note that $a \to 0$ implies $\theta \to 0$. We will also use the observation that

$$\lim_{a\to 0} \frac{1}{a}(u^2 + O(u^3)) = \lim_{a\to 0} \frac{1}{a}(av^2 + a^{\frac{3}{2}}O(v^3)) = v^2$$

and

$$\lim_{a\to 0} \frac{1}{a}(\sin\theta u) = \lim_{a\to 0} \frac{1}{a}(\cos\theta a^{1-\beta+\frac{1}{2}}v) = \lim_{a\to 0} a^{\frac{1}{2}-\beta}\cos\theta v) = 0.$$

With these observations, it now follows that

$$\begin{aligned}
\lim_{a\to 0^+} 2\pi i a^{1-\frac{\beta}{2}} I_{10}(a,0,0) &= \int_0^\infty \hat{\psi_1}(\rho) \int_{-1}^1 \hat{\psi}_2(t) \int_{-\infty}^\infty e^{-2\pi i\rho v^2}\, dv\, dt\, d\rho\\
&\quad + \int_0^\infty \hat{\psi_1}(\rho) \int_{-1}^1 \hat{\psi}_2(t) \int_{-\infty}^\infty e^{2\pi i\rho v^2}\, dv\, dt\, d\rho\\
&= \int_0^\infty \frac{\hat{\psi}_1(\rho)}{\sqrt{\rho}} d\rho \int_{-1}^1 \hat{\psi}_2(t)\, dt > 0.
\end{aligned}$$

This completes the proof of part (iv).

• *Part (v)* We need only to consider $\frac{1}{2} < \beta < 1$.

Here again we let $t = a^{\beta-1}\tan\theta$, but let $u = a^\beta v$ as in the proof of part (iii) (recall that we let $u = a^{\frac{1}{2}}v$ in the proof of part (iv)). In this case we have

$$\lim_{a\to 0} \frac{1}{a}(u^2 + O(u^3)) = \lim_{a\to 0} \frac{1}{a}(a^{2\beta}v^2 + a^{3\beta}O(v^3)) = 0$$

$$\lim_{a\to 0}\frac{1}{a}(\sin\theta\ u)=\lim_{a\to 0}\frac{1}{a}(\cos\theta\ a^{1-\beta+\beta}tv)=t\ v.$$

Following the same argument as in the proof of part (iii), we have

$$\begin{aligned}\lim_{a\to 0^+} 2\pi i a^{-\frac{1+\beta}{2}} I_{10}(a,0,0) &= \int_0^\infty \psi_1\hat{(}\rho)\int_{-\infty}^{\infty}\int_{-1}^{1}\hat{\psi}_2(t)e^{-2\pi i\rho vt}\,dt\,dv\,d\rho\\ &+\int_0^\infty \hat{\psi}_1(\rho)\int_{-\infty}^{\infty}\int_{-1}^{1}\hat{\psi}_2(t)e^{2\pi i\rho vt}\,dt\,dv\,d\rho\\ &=2\hat{\psi}_2(0)\int_0^\infty\hat{\psi}_1(\rho)\,d\rho>0.\end{aligned}$$

4 Shearlet analysis of edges in dimension $n=3$

The shearlet-based analysis of step edges we presented above extends to the 3-dimensional setting [20, 21]. The statements of the 3D results are formally very similar to their 2-dimensional counterparts. Also the proofs follow essentially the same ideas of the 2D case, except for more significant changes needed for the analysis of the irregular boundary points. Indeed, if we consider functions of the form $f=\chi_\Omega$ where $\Omega\subset\mathbb{R}^3$ is a compact set with piecewise smooth boundary, then there are two main types of 'edges' to consider: the smooth (or regular) surface boundaries and the curvilinear singularities resulting from the intersection of different smooth (or regular) sections of such surfaces. We will show below that it is possible to design an appropriate modification of the continuous shearlet transform suited to these curvilinear singularities in $\mathbb{R}^3$.

4.1 3D Continuous Shearlet Transform

There is a natural way to extend to the 3D setting the 2-dimensional fine-scale continuous shearlet transform we constructed in Section 2.3. Similar to the 2-dimensional case, we can define separate 3D shearlet systems spanning proper subspaces of $L^2(\mathbb{R}^3)$, which are obtained by restricting the shear variables to a finite subset only. Namely, we introduce the following pyramidal regions in $\mathbb{R}^3$:

$$\begin{aligned}\mathscr{P}_1&=\{(\xi_1,\xi_2,\xi_3)\in\mathbb{R}^3:|\xi_1|\geq 2,\ |\tfrac{\xi_2}{\xi_1}|\leq 1 \text{ and } |\tfrac{\xi_3}{\xi_1}|\leq 1\},\\ \mathscr{P}_2&=\{(\xi_1,\xi_2,\xi_3)\in\mathbb{R}^3:|\xi_2|\geq 2,\ |\tfrac{\xi_2}{\xi_1}|> 1 \text{ and } |\tfrac{\xi_3}{\xi_2}|\leq 1\},\\ \mathscr{P}_3&=\{(\xi_1,\xi_2,\xi_3)\in\mathbb{R}^3:|\xi_3|\geq 2,\ |\tfrac{\xi_3}{\xi_1}|> 1 \text{ and } |\tfrac{\xi_3}{\xi_2}|> 1\}.\end{aligned}$$

For $\xi=(\xi_1,\xi_2,\xi_3)\in\mathbb{R}^3$, $\xi_1\neq 0$, let $\psi^{(d)}$, $d=1,2,3$ be defined by

$$\hat{\psi}^{(1)}(\xi) = \hat{\psi}^{(1)}(\xi_1,\xi_2,\xi_3) = \hat{\psi}_1(\xi_1)\,\hat{\psi}_2(\tfrac{\xi_2}{\xi_1}),\hat{\psi}_2(\tfrac{\xi_3}{\xi_1}),$$
$$\hat{\psi}^{(2)}(\xi) = \hat{\psi}^{(2)}(\xi_1,\xi_2,\xi_3) = \hat{\psi}_1(\xi_2)\,\hat{\psi}_2(\tfrac{\xi_1}{\xi_2}),\hat{\psi}_2(\tfrac{\xi_3}{\xi_2}),$$
$$\hat{\psi}^{(3)}(\xi) = \hat{\psi}^{(3)}(\xi_1,\xi_2,\xi_3) = \hat{\psi}_1(\xi_3)\,\hat{\psi}_2(\tfrac{\xi_2}{\xi_3}),\hat{\psi}_2(\tfrac{\xi_1}{\xi_3}),$$

where ψ_1, ψ_2 satisfy the same assumptions as in the 2D case. For $d = 1,2,3$, and $\beta = (\beta_1,\beta_2)$, with $0 < \beta_1,\beta_2 < 1$, the *3D pyramid-based continuous shearlet systems for* $L^2(\mathscr{P}_d)^\vee$ are the systems

$$\{\psi^{(d)}_{a,s_1,s_2,t} : 0 \le a \le \tfrac{1}{4}, -\tfrac{3}{2} \le s_1 \le \tfrac{3}{2}, -\tfrac{3}{2} \le s_2 \le \tfrac{3}{2}, t \in \mathbb{R}^3\},$$

where $\psi^{(d)}_{a,s_1,s_2,t}(x) = |\det M^{(d)}_{as_1s_2}|^{-\frac{1}{2}}\,\psi^{(d)}((M^{(d)}_{as_1s_2})^{-1}(x-t))$, and

$$M^{(1)}_{as_1s_2} = \begin{pmatrix} a & -a^{\beta_1}s_1 & -a^{\beta_2}s_2 \\ 0 & a^{\beta_1} & 0 \\ 0 & 0 & a^{\beta_2} \end{pmatrix},\quad M^{(2)}_{as_1s_2} = \begin{pmatrix} a^{\beta_1} & 0 & 0 \\ -a^{\beta_1}s_1 & a & -a^{\beta_2}s_2 \\ 0 & 0 & a^{\beta_2} \end{pmatrix},$$

$$M^{(3)}_{as_1s_2} = \begin{pmatrix} a^{\beta_1} & 0 & 0 \\ 0 & a^{\beta_2} & 0 \\ -a^{\beta_1}s_1 & -a^{\beta_2}s_2 & a \end{pmatrix}.$$

In particular, in the Fourier domain, the shearlets $\psi^{(1)}_{a,s_1,s_2,t}$ have the form:

$$\hat{\psi}^{(1)}_{a,s_1,s_2,t}(\xi_1,\xi_2,\xi_3) = a^{\frac{1+\beta_1+\beta_2}{2}}\,\hat{\psi}_1(a\,\xi_1)\,\hat{\psi}_2(a^{\beta_1-1}(\tfrac{\xi_2}{\xi_1}-s_1))\,\hat{\psi}_2(a^{\beta_2-1}(\tfrac{\xi_3}{\xi_1}-s_2))\,e^{-2\pi i\xi\cdot t},$$

with similar expressions for the shearlets on the other pyramidal regions. This shows that, similar to the 2D case, the shearlets $\psi^{(d)}_{a,s_1,s_2,t}$ are well localized waveforms associated with various scales controlled by a, orientations controlled by the two shear variables s_1,s_2 and locations controlled by t. Fig. 3 shows the Fourier domain support of a representative element of a 3D continuous shearlet system.

For $f \in L^2(\mathbb{R}^3)$, we define the *3D (fine-scale) pyramid-based continuous shearlet transform* $f \to \mathscr{SH}_\psi f(a,s_1,s_2,t)$, for $a > 0$, $s_1,s_2 \in \mathbb{R}$, $t \in \mathbb{R}^3$ by

$$\mathscr{SH}_\psi f(a,s_1,s_2,t) = \begin{cases} \langle f, \psi^{(1)}_{a,s_1,s_2,t}\rangle & \text{if } |s_1|,|s_2| \le 1, \\ \langle f, \psi^{(2)}_{a,\frac{1}{s_1},\frac{s_2}{s_1},t}\rangle & \text{if } |s_1| > 1, |s_2| \le |s_1| \\ \langle f, \psi^{(3)}_{a,\frac{s_1}{s_2},\frac{1}{s_2},t}\rangle & \text{if } |s_2| > 1, |s_2| > |s_1|. \end{cases}$$

That is, depending on the values of the shearing variables, the 3D continuous shearlet transform only involves one specific pyramid-based shearlet system. As above, we are only interested in the continuous shearlet transform at"fine scales", as a approaches 0, since this is what is needed for the analysis of the singularities of f.

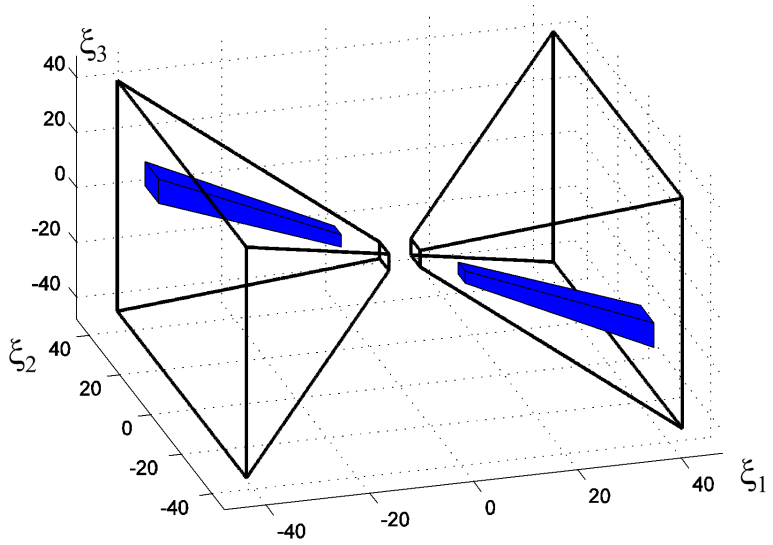

Fig. 3 Fourier domain support of a representative element $\psi^{(1)}_{a,s_1,s_2,t}$ of a 3D continuous shearlet system, inside the pyramidal region $\mathscr{P}_1$.

4.2 Characterization of 3D Boundaries

Similar to its 2D counterpart, the 3D continuous shearlet transform can be applied to analyze the geometry of the set of singularities of functions and distributions of 3 variables. In particular, we can show that it provides a geometric characterization of the boundary set of a solid regions.

To state the precise result, let $f = \chi_\Omega$, where Ω is a subset of $\mathbb{R}^3$ whose boundary $\partial\Omega$ is a 2-dimensional manifold. We say that $\partial\Omega$ is *piecewise smooth* if:

(i) $\partial\Omega$ is a C^∞ manifold except possibly for finitely many separating C^3 curves on $\partial\Omega$;
(ii) at each point on a separating curve, $\partial\Omega$ has exactly two outer normal vectors, which are not on the same line.

Let the outer normal vector of $\partial\Omega$ be $\mathbf{n}_p = \pm(\cos\theta_0 \sin\phi_0, \sin\theta_0 \sin\phi_0, \cos\phi_0)$ for some $\theta_0 \in [0, 2\pi]$, $\phi_0 \in [0, \pi]$. We say that $s = (s_1, s_2)$ corresponds to the normal direction $\mathbf{n}_p$ if $s_1 = a^{-\frac{1}{2}} \tan\theta_0$, $s_2 = a^{-\frac{1}{2}} \cot\phi_0 \sec\theta_0$. Notice that this definition excludes, in particular, surfaces containing cusps, such as the vertex of a cone.

The following theorem, which is a proved in [21], shows that the behaviour of the 3D continuous shearlet transform is consistent with the one found in dimension $n = 2$. Namely, for $f = \chi_\Omega$, the continuous shearlet transform $\mathscr{SH}_\psi f(a, s_1, s_2, t)$, has rapid asymptotic decay as $a \to 0$ for all locations $t \in \mathbb{R}^3$, except when t is on the boundary of Ω and the orientation variables s_1, s_2 correspond to the normal direction of the boundary surface at t, or when t is on a separating curve and the orientation

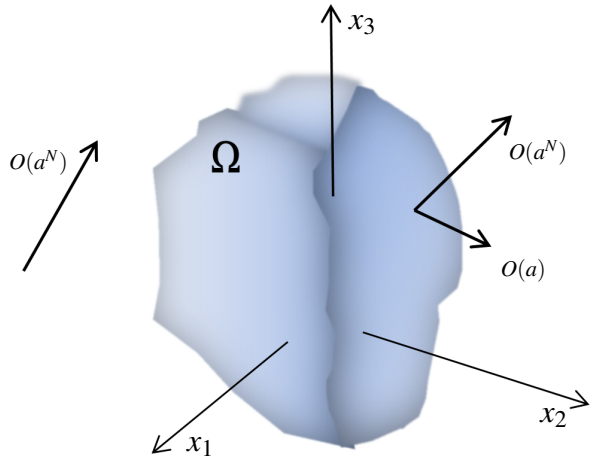

Fig. 4 Asymptotic decay rate of the 3D continuous shearlet transform. The continuous shearlet transform $\mathscr{SH}_\psi B(a,s_1,s_2,t)$, where $B=\chi_\Omega$, $\Omega\subset\mathbb{R}^3$ and $\partial\Omega$ piecewise smooth boundary has rapid asymptotic decay, as $a\to 0$, away from $\partial\Omega$. When $t\in\partial\Omega$ is a regular boundary point and the shear variables (s_1,s_2) correspond to the normal direction at t, then $\mathscr{SH}_\psi B(a,s_1,s_2,t)\sim O(a)$, as $a\to 0$; otherwise, if (s_1,s_2) does not correspond to the normal direction at t, $\mathscr{SH}_\psi B$ has rapid asymptotic decay.

variables s_1,s_2 correspond to the normal direction of the boundary surface at t. Thus, as in the 2D case, the continuous shearlet transform provides a description of the geometry of $\partial\Omega$ through the asymptotic decay of $\mathscr{SH}_\psi B(a,s_1,s_2,t)$, at fine scales. Here is the precise statement for the case $\beta_1=\beta_2=\frac{1}{2}$.

Theorem 3. *Let ψ_1 ψ_2 be chosen as in Theorem 1, $\beta_1=\beta_2=\frac{1}{2}$ and $f=\chi_\Omega$, where Ω be a bounded region in $\mathbb{R}^3$. Assume that the boundary surface $\partial\Omega$ is a piecewise smooth 2-dimensional manifold. Let γ_j, $j=1,2,\cdots m$ be the separating curves of $\partial\Omega$. Then we have*

(i) If $t\notin\partial\Omega$ then

$$\lim_{a\to 0^+} a^{-N}\,\mathscr{SH}_\psi f(a,s_1,s_2,t)=0,\quad \text{for all } N>0.$$

(ii) If $t\in\partial\Omega\setminus\bigcup_{j=1}^m\gamma_j$ and (s_1,s_2) does not correspond to the normal direction of $\partial\Omega$ at t, then

$$\lim_{a\to 0^+} a^{-N}\,\mathscr{SH}_\psi f(a,s_1,s_2,t)=0,\quad \text{for all } N>0.$$

(iii) If $t\in\partial\Omega\setminus\bigcup_{j=1}^m\gamma_j$ and $s=(s_1,s_2)$ corresponds to the normal direction of $\partial\Omega$ at t or $t\in\bigcup_{j=1}^m\gamma_j$ and $s=(s_1,s_2)$ corresponds to one of the two normal directions of $\partial\Omega$ at t, then

$$\lim_{a\to 0^+} a^{-1}\,\mathscr{SH}_\psi f(a,s_1,s_2,t)\neq 0.$$

Hence, similar to the 2D case, the continuous shearlet transform decays rapidly away from the boundary and on the boundary for non-normal orientations. The decay rate is only $O(a)$ at the boundary for normal orientation. This behavior illustrated in Fig. 4. On the separating curves of the surface γ_i the information provided by the theorem is less sharp, in the sense that, for normal orientations, the decay rate is $O(a)$, but, for non-normal orientations, we can only say that the decay rate is faster but not necessarily rapid. In particular, it is shown in [21] that, when $\beta_1 = \beta_2 = 1/2$, the decay rate is of order $O(a^{3/2})$ or faster. We will see in Section 4.3 that there is an alternative and more precise approach to analyze the curves γ_i.

We refer the reader to [21] for the complete proof of Theorem 3. In the following, we make a few basic observation about this proof.

As in the 2D case, the starting point of the proof is the divergence theorem, which allows us to write the Fourier transform of f as

$$\hat{f}(\xi) = \widehat{\chi}_\Omega(\xi) = -\frac{1}{2\pi i|\xi|^2}\int_{\partial\Omega} e^{-2\pi i\xi\cdot x}\,\xi\cdot\mathbf{n}(x)\,d\sigma(x),$$

where $\mathbf{n}$ is the outer normal vector to $\partial\Omega$ at x. Next, using spherical coordinates, we have that, for $|s_1|, |s_2| < 1$,

$$\mathscr{SH}_\psi f(a,s_1,s_2,t) = \langle f, \psi^{(1)}_{a,s_1,s_2,t}\rangle = I_1(a,s_1,s_2,t) + I_2(a,s_1,s_2,t),$$

where

$$I_1(a,s_1,s_2,t) = \int_0^{2\pi}\int_0^{\pi}\int_0^{\infty} T_1(\rho,\theta,\phi)\,\overline{\hat{\psi}^{(1)}_{a,s_1,s_2,t}}(\rho,\theta,\phi)\,\rho^2\sin\phi\,d\rho\,d\phi\,d\theta$$
$$I_2(a,s_1,s_2,t) = \int_0^{2\pi}\int_0^{\pi}\int_0^{\infty} T_2(\rho,\theta,\phi)\,\overline{\hat{\psi}^{(1)}_{a,s_1,s_2,t}}(\rho,\theta,\phi)\,\rho^2\sin\phi\,d\rho\,d\phi\,d\theta$$

and

$$T_1(\rho,\theta,\phi) = -\frac{1}{2\pi i\rho}\int_{P_\varepsilon(t)} e^{-2\pi i\rho\,\Theta(\theta,\phi)\cdot x}\,\Theta(\theta,\phi)\cdot\mathbf{n}(x)\,d\sigma(x)$$
$$T_2(\rho,\theta,\phi) = -\frac{1}{2\pi i\rho}\int_{\partial\Omega\setminus P_\varepsilon(t)} e^{-2\pi i\rho\,\Theta(\theta,\phi)\cdot x}\,\Theta(\theta,\phi)\cdot\mathbf{n}(x)\,d\sigma(x),$$

where $P_\varepsilon(t) = \partial\Omega\cap D(\varepsilon,t)$, and $D(\varepsilon,t)$ is the ball in $\mathbb{R}^3$ of radius ε and center t. Notice that I_2 is associated with the term T_2 which is evaluated away from the location t of the continuous shearlet transform. Hence, a localization result similar to Lemma 1 shows that I_2 is rapidly decreasing as $a\to 0$. The rest of the proof, when t is located on a regular point of $\partial\Omega$, can be derived using ideas similar to the proof of Theorem 1. The situation for t located on a separating curve requires a different approach cannot be carried out using the method from the proof of Theorem 2.

4.3 Identification of curve singularities on the piecewise smooth surface boundary of a solid

In the 3-dimensional setting, there are other types of singularities of interest beside the surface boundary of a solid region. In particular, if $f = \chi_\Omega$, where $\Omega \subset \mathbb{R}^3$ is a compact subset whose surface boundary $S_\Omega = \partial\Omega$ is the union $S_\Omega = \cup_{i=1}^q S_i$ and each S_i is a smooth surface with boundary curve γ_i, it may be useful to identify the location and orientation of the separating curves $\gamma = \gamma_1 \cup \cdots \cup \gamma_m$.

We can attempt to address this question by making use of the results of Section 4.2 to determine if a given $t \in \mathbb{R}^3$ belongs to γ, and, if so, the value of $\gamma'|_t$. Using Theorem 3, where we choose $\beta_1 = \beta_2 = 1/2$, we make the following observations.

- If $a^{-N} \lim_{a\to 0^+} \mathcal{SH}_\psi f(a,s_1,s_2,t) = 0$, for all $N > 0$ and all but at most one pair (s_1,s_2), then $t \notin \gamma$.
- If $a^{-N_k} \lim_{a\to 0^+} \mathcal{SH}_\psi f(a,s_1^k,s_2^k,t) \neq 0$ for some $N_0, N_1 > 0$ and distinct (s_1^0,s_2^0) and (s_1^1,s_2^1), then $t \in \gamma$.
- If $a^{-1} \lim_{a\to 0^+} \mathcal{SH}_\psi f(a,s_1^k,s_2^k,t) \neq 0$ for distinct (s_1^0,s_2^0) and (s_1^1,s_2^1) then $\gamma'|_t$ equals (up to a scalar) the vector cross product of the orientations corresponding to (s_1^0,s_2^0) and (s_1^1,s_2^1).

However, there are multiple drawbacks regarding the applicability of this method. First, suppose $\mathcal{SH}_\psi f(a,s_1,s_2,t)$ is observed to decay relatively slowly as $a \to 0^+$ for all (s_1,s_2) only in some localized directional region S. It may be difficult to determine whether there is a single peak of slow decay (s_1^0,s_2^0) (indicating $t \notin \gamma$) or two nearby peaks of slow decay (s_1^0,s_2^0) and (s_1^1,s_2^1) (indicating $t \in \gamma$). Second, suppose we are relatively certain that $t \in \gamma$. To determine $\gamma'|_t$, we need to determine the two values (s_1^0,s_2^0) and (s_1^1,s_2^1) such that

$$a^{-1} \lim_{a\to 0^+} \mathcal{SH}_\psi f(a,s_1^k,s_2^k,t) \neq 0,$$

for $k = 1,2$. However, (s_1^0,s_2^0) and (s_1^1,s_2^1) may be difficult to isolate since, by Theorem 3, there may be $(s_1,s_2) \neq (s_1^0,s_2^0),(s_1^1,s_2^1)$ with comparably slow decay rates:

$$a^{-3/2} \lim_{a\to 0^+} \mathcal{SH}_\psi f(a,s_1,s_2,t) \neq 0.$$

As an alternative approach to this problem, one can introduce a modified continuous shearlet transform that can precisely address the question posed in the first paragraph of this section, while avoiding all of the limitations suggested in the previous paragraph. This idea was recently introduced in [28], and we summarized the main result below.

First, let us be more precise about the types of objects we will consider. We say that the surface boundary S_Ω of Ω is piecewise C^K at t if there exists an open set $U \subset \mathbb{R}^3$ with $t \in U$ and $F,G \in C^K(U,\mathbb{R})$ with $F(t) = G(t) = 0$ and $\{\nabla F(t), \nabla G(t)\}$ linearly independent such that

$$\Omega \cap U = \{x \in U : F(x) < 0\} \square \{x \in U : G(x) < 0\}$$

(in the a.e. sense), where the symbol $\square$ can be either $\cap$ or $\cup$. In this case, we call

$$\mathscr{O}_\Omega(t) = \nabla F(t) \times \nabla G(t)$$

(where $\times$ is the vector cross product) the orientation of S_Ω at t. Note that $\mathscr{O}_\Omega(t)$ is well-defined (up to nonzero scalar multiplication) and equals the *tangent vector* at t to the curve defined by $\{x : F(x) = G(x) = 0\}$ near t.

Fix $\beta_1 > \beta_3 > \beta_2 > 0$ and write $\beta_0 = (\beta_1 - \beta_2 - \beta_3)/2$. For $a > 0$ and $s \in \mathbb{R}$, we define the following matrices:

$$B_{21}(s) = \begin{pmatrix} 1 & 0 & 0 \\ s & 1 & 0 \\ 0 & 0 & 1 \end{pmatrix} \quad B_{12}(s) = \begin{pmatrix} 1 & s & 0 \\ 0 & 1 & 0 \\ 0 & 0 & 1 \end{pmatrix} \quad B_{13}(s) = \begin{pmatrix} 1 & 0 & s \\ 0 & 1 & 0 \\ 0 & 0 & 1 \end{pmatrix}$$

$$B_{31}(s) = \begin{pmatrix} 1 & 0 & 0 \\ 0 & 1 & 0 \\ s & 0 & 1 \end{pmatrix} \quad B_{32}(s) = \begin{pmatrix} 1 & 0 & 0 \\ 0 & 1 & 0 \\ 0 & s & 1 \end{pmatrix} \quad B_{23}(s) = \begin{pmatrix} 1 & 0 & 0 \\ 0 & 1 & s \\ 0 & 0 & 1 \end{pmatrix}$$

$$A_{21}(a) = \begin{pmatrix} a^{\beta_3} & 0 & 0 \\ 0 & a^{\beta_1} & 0 \\ 0 & 0 & a^{\beta_2} \end{pmatrix} A_{12}(a) = \begin{pmatrix} a^{\beta_1} & 0 & 0 \\ 0 & a^{\beta_3} & 0 \\ 0 & 0 & a^{\beta_2} \end{pmatrix} A_{13}(a) = \begin{pmatrix} a^{\beta_1} & 0 & 0 \\ 0 & a^{\beta_2} & 0 \\ 0 & 0 & a^{\beta_3} \end{pmatrix}$$

$$A_{31}(a) = \begin{pmatrix} a^{\beta_3} & 0 & 0 \\ 0 & a^{\beta_2} & 0 \\ 0 & 0 & a^{\beta_1} \end{pmatrix} A_{32}(a) = \begin{pmatrix} a^{\beta_2} & 0 & 0 \\ 0 & a^{\beta_3} & 0 \\ 0 & 0 & a^{\beta_1} \end{pmatrix} A_{23}(a) = \begin{pmatrix} a^{\beta_2} & 0 & 0 \\ 0 & a^{\beta_1} & 0 \\ 0 & 0 & a^{\beta_3} \end{pmatrix}$$

$$\sigma_{21} = \begin{pmatrix} 0 & 0 & 1 \\ 1 & 0 & 0 \\ 0 & 1 & 0 \end{pmatrix} \quad \sigma_{12} = \begin{pmatrix} 1 & 0 & 0 \\ 0 & 0 & 1 \\ 0 & 1 & 0 \end{pmatrix} \quad \sigma_{13} = \begin{pmatrix} 1 & 0 & 0 \\ 0 & 1 & 0 \\ 0 & 0 & 1 \end{pmatrix}$$

$$\sigma_{31} = \begin{pmatrix} 0 & 0 & 1 \\ 0 & 1 & 0 \\ 1 & 0 & 0 \end{pmatrix} \quad \sigma_{32} = \begin{pmatrix} 0 & 1 & 0 \\ 0 & 0 & 1 \\ 1 & 0 & 0 \end{pmatrix} \quad \sigma_{23} = \begin{pmatrix} 0 & 1 & 0 \\ 1 & 0 & 0 \\ 0 & 0 & 1 \end{pmatrix}.$$

Let $\psi \in L^2(\mathbb{R}^3)$, and, for $t \in \mathbb{R}^3$, define

$$\psi^{ij}_{a,s,t} = |\det A_{ij}^{-1}|\, \psi(\sigma_{ij}^{-1} A_{ij}^{-1} B_{ij}^{-1}(x-t)). \tag{16}$$

The collection $\{\psi^{ij}_{a,s,t}\}$ induces the 6 continuous transforms $\{\mathscr{S}^{ij}\}$, where

$$\mathscr{S}^{ij} f(a,s,t) = \langle f, \psi^{ij}_{a,s,t} \rangle.$$

We are now ready to define a new transform able to capture curvilinear singularities on the surface of a solid in 3D. Let $\mathbb{V}$ denote $(\mathbb{R}^3 \setminus \{0\})/\sim$, where $v \sim w$ if $v = cw$ for some $c \in \mathbb{R} \setminus \{0\}$. Write

$$\mathscr{K} = \{(2,1),(3,1),(1,2),(3,2),(1,3),(2,3)\}$$

and, for $(i,j) \in \mathscr{K}$, define

$$\mathscr{P}_{ij} = \begin{cases} [-1,1], & \text{if } (i,j) = (1,3),(2,3),(1,2) \\ (-1,1), & \text{otherwise} \end{cases}.$$

If $v \in \mathbb{V}$, there exists a unique $j = j(v) \in \{1,2,3\}$ such that $v_j \neq 0$ and $v_i/v_j \in \mathscr{P}_{ij}$, for all i, with the quantities j and v_i/v_j well-defined with respect to $\sim$. If $a > 0$, $v \in \mathbb{V}$, and $t \in \mathbb{R}^3$, we define the $(3,1)$-*continuous shearlet transform* $\mathscr{S}_{(3,1)}$ as

$$\mathscr{S}_{(3,1)} f(a,v,t) = \prod_{i \in \{1,2,3\} \setminus \{j\}} S_{ij} f(a, v_i/v_j, t).$$

The "$(3,1)$" indicates that the transform is designed to capture singularities along 1-dimensional structures in the 3-dimensional ambient space.

Before stating the main theorem from [28], we will make some additional assumptions on ψ given by (16).

Let $0 < \varepsilon < M_1 < \infty$ and $0 < M_2 < M_3 < \infty$ be such that

$$\frac{M_3}{M_2} > \left(\frac{M_1}{\varepsilon}\right)^{\beta_2/\beta_1}.$$

Choose $\theta_1, \theta_2 \in C^\infty(\mathbb{R})$ such that

$$\operatorname{supp}(\theta_1) \subset [\varepsilon, M_1], \quad \int_0^\infty \theta_1(a)^2 \frac{da}{a} = \beta_1/2,$$

θ_2 is compactly supported in $(0,\infty)$, and

$$|\theta_2(\xi)| = 1, \quad \text{for all } M_2 \leq \xi \leq M_3.$$

For $q = 1,2$, define

$$\theta_q^{\text{even}}(\xi) = \begin{cases} \theta_q(\xi), & \text{if } \xi \geq 0 \\ \theta_q(-\xi), & \text{if } \xi < 0 \end{cases},$$

$$\theta_q^{\text{odd}}(\xi) = \begin{cases} \theta_q(\xi), & \text{if } \xi \geq 0 \\ -\theta_q(-\xi), & \text{if } \xi < 0 \end{cases},$$

and $\psi_q \in L^2(\mathbb{R})$ by $\hat{\psi}_q = \theta_q^{\text{even}} + i\theta_q^{\text{odd}}$. Let $0 < M_4 < \infty$ and choose $\psi_3 \in L^2(\mathbb{R})$ such that $\hat{\psi}_3$ is even, belongs to $C^\infty(\mathbb{R},\mathbb{R})$, and satisfies $\hat{\psi}_3(0) \neq 0$,

$$\operatorname{supp}(\hat{\psi}_3) \subset [-M_4, M_4], \quad \text{and} \quad \|\psi_3\| = 1.$$

Finally, define $\psi \in L^2(\mathbb{R}^3)$ by $\hat{\psi}(\xi) = \hat{\psi}_1(\xi_1)\hat{\psi}_2(\xi_2)\hat{\psi}_3(\xi_3/\xi_1)$. Note, in particular, that ψ is real-valued and that $\hat{\psi}$ belongs to $C^\infty(\mathbb{R}^3)$ and is compactly supported.

With this choice of ψ we can now state the following result[2], which shows that $\mathscr{S}_{(3,1)}$ precisely identifies both t and the tangent vector $\mathscr{O}_\Omega(t)$ when S_Ω is piecewise C^∞ at t.

Theorem 4. *Let $f = \chi_\Omega$ and suppose that $\beta_1 < 2\beta_2$. We have the following:*

- *If $t \notin \overline{S_\Omega}$, where $\overline{S_\Omega}$ denotes the closure of S_Ω, or if S_Ω is C^∞ at t, then*

$$\lim_{a\to 0^+} a^{-N}\mathscr{S}_{(3,1)}f(a,v,t) = 0,$$

  for all $N > 0$ and all $v \in \mathbb{V}$.
- *Let $v \in \mathbb{V}$ and assume S_Ω is piecewise C^∞ at p. If $v \sim \mathscr{O}_\Omega(t)$, then*

$$\lim_{a\to 0^+} a^{-2(\beta_1+\beta_3+\beta_0)}\mathscr{S}_{(3,1)}f(a,v,t) \in \mathbb{C}\cup\{\infty\}\setminus\{0\};$$

  otherwise,

$$\lim_{a\to 0^+} a^{-N}\mathscr{S}_{(3,1)}(\Omega)(a,v,t) = 0,$$

  for all $N > 0$.

We refer to [28] for a discussion of more technical aspects of the theorems, such as the assumptions on the analyzing functions, and for the proof of this result. In the following, we will briefly illustrate the application of Theorem 4 using a simple example.

We set $f = \chi_\Omega$ where

$$\Omega \cap U = \{x \in U : x_1 < 0\} \cap \{x \in U : x_2 < 0\},$$

and $U = (-1,1)^3$. Write $\Gamma = \{x \in U : x_1 = x_2 = 0\}$,

$$S_1 = \{x \in U : x_1 = 0, x_2 < 0\}, \quad \text{and} \quad S_2 = \{x \in U : x_1 < 0, x_2 = 0\}.$$

Then, it follows that

- $\overline{S_\Omega} \cap U = S_1 \cup \Gamma \cup S_2$
- S_Ω is C^∞ at t, for all $t \in S_1 \cup S_2$
- S_Ω is piecewise C^∞ at t, with $\mathscr{O}_\Omega(t) = (0,0,1)$ and $j(\mathscr{O}_\Omega(t)) = 3$, for all $t \in \Gamma$.

Thus, Theorem 4 implies that

- If $t \in U \setminus \Gamma$, then

$$\lim_{a\to 0^+} a^{-N}\mathscr{S}_{(3,1)}(\Omega)(a,v,t) = 0,$$

  for all $N > 0$ and all $v \in \mathbb{V}$.

[2] Note that, in [28], the theorem is stated under more general assumptions on ψ satisfying an appropriate admissibility condition. The special function we consider here is in fact one example of a function satisfying such admissibility condition.

- Assume $t \in \Gamma$. If $v \sim (0,0,1)$,

$$\lim_{a\to 0^+} a^{-2(\beta_1+\beta_3+\beta_0)} \mathscr{S}_{(3,1)} f(a,v,t) \in \mathbb{C} \cup \{\infty\} \setminus \{0\};$$

otherwise,

$$\lim_{a\to 0^+} a^{-N} \mathscr{S}_{(3,1)} f(a,v,t) = 0, \tag{17}$$

for all $N > 0$.

Thus, the (3,1)-continuous shearlet transform characterizes both the location and orientation of the singularity curve Γ through its asymptotic decay at fine scales.

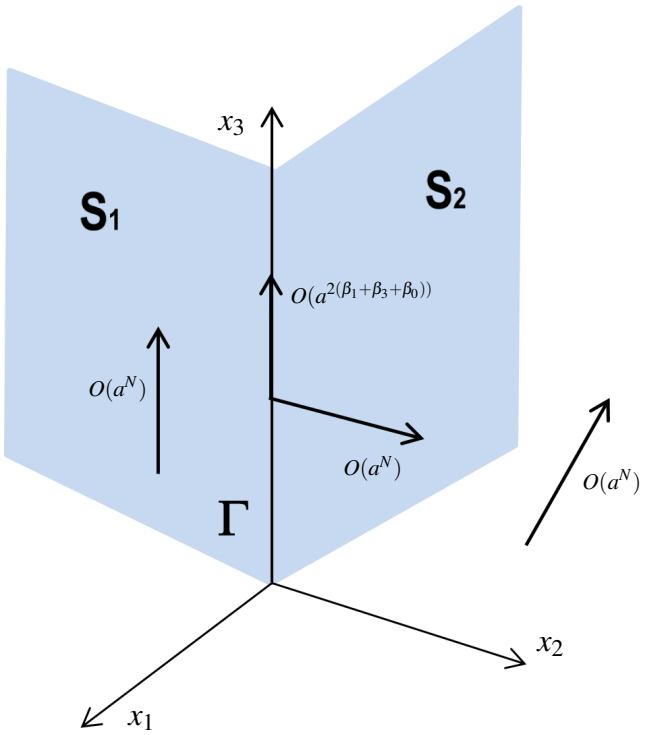

Fig. 5 Asymptotic decay rate of the (3,1)-continuous shearlet transform $\mathscr{S}_{(3,1)}$ of $f = \chi_\Omega$, where $\Omega \subset \mathbb{R}^3$ has piecewise smooth boundary $S = S_1 \cup S_2 \cup \ldots$. Away from the surface S and on S but away from Γ, the decay is faster than $O(a^N)$, for any $N \in \mathbb{N}$. When $t \in \Gamma$, for v corresponding to the tangent direction of Γ at t, $\mathscr{S}_{(3,1)} f(a,v,t)$ decays as $O(a^{2(\beta_1+\beta_3+\beta_0)})$; when v does not correspond to the tangent direction of Γ at t, the decay is faster than $O(a^N)$, for any $N \in \mathbb{N}$.

On the other hand, one can verify that the 'standard' 3D continuous shearlet transform $\mathscr{SH}_\psi$ defined in Section 4.1 is not very efficient to capture the geometry of the singularity line Γ. In fact we observe the following.

- If $t \in U \setminus (\Gamma \cup S_1 \cup S_2)$, then

$$\lim_{a\to 0^+} a^{-N} \mathscr{SH}_\psi f(a,v,t) = 0,$$

for all $v \in \mathbb{V}$ and all $K > 0$.
- Assume $p \in S_1$. If $v = (1,0,0)$ (i.e., the normal vector of S_1), then

$$\lim_{a\to 0^+} a^{-1} \mathscr{SH}_\psi f(a,v,t) \neq 0;$$

otherwise,

$$\lim_{a\to 0^+} a^{-N} \mathscr{SH}_\psi f(a,v,t) = 0,$$

for all $N > 0$.
- Assume $t \in S_2$. If $v = (0,1,0)$ (i.e., the normal vector of S_2), then

$$\lim_{a\to 0^+} a^{-1} \mathscr{S}_{(3,2)}(\Omega)(a,v,t) \neq 0;$$

otherwise,

$$\lim_{a\to 0^+} a^{-N} \mathscr{S}_{(3,2)}(\Omega)(a,v,t) = 0,$$

for all $N > 0$.
- Assume $t \in \Gamma$. If $v \in \{(1,0,0),(0,1,0)\}$, then

$$\lim_{a\to 0^+} a^{-1} \mathscr{SH}_\psi f(a,v,t) \neq 0;$$

otherwise,

$$\limsup_{a\to 0^+} a^{-3/2} \mathscr{SH}_\psi f(a,v,t) < \infty. \tag{18}$$

We thus see that $\mathscr{SH}_\psi f$ is able to detect the location of Γ as all t such that the condition

$$\lim_{a\to 0^+} \alpha^{-N} \mathscr{SH}_\psi f(a,v,t) = 0, \text{ for all } N > 0$$

fails for two at least two v. In this case, $\mathscr{SH}_\psi f$ can then detect the orientation, $(0,0,1)$, of Γ as the vector cross product of the two unique v, $(1,0,0)$ and $(0,1,0)$, for which (18) fails. Comparing these results to the those in the previous paragraph (particularly, (17) to (18)), we see that while $\mathscr{SH}_\psi f$ can detect the location of Γ just as precisely as $\mathscr{S}_{(3,1)}$, the latter is much better able to precisely identify the orientation of Γ.

5 Other results and applications

The shearlet analysis of singularities extends beyond the cases considered in the previous sections. In this section, we will briefly review the results available in the

literature. We will also include a brief discussion of the numerical algorithms that were developed based on shearlet analysis of singularities.

5.1 Shearlet analysis of general edges

In the engineering literature, it is common to consider several types of edges beside the step edges [43]. For example, ramp edges are associated with sharp linear transitions in images. As an idealized model of such edges, let as consider the two-dimensional distribution $x_1H(x_1,x_2)$, where H is the two-dimensional Heaviside step function defined in Section 1. The line $x_1 = 0$ is the ramp edge that we wish to detect.

By applying the continuous shearlet transform, a calculation very similar to Section 1 yields:

$$\begin{aligned}
&\mathcal{SH}_\psi(x_1H)(a,s,t) = \langle x_1H, \psi_{a,s,t}\rangle \\
&= -\frac{1}{2\pi i}\int_{\mathbb{R}^2} \partial_1\hat{H}(\xi_1,\xi_2)\,\overline{\hat{\psi}_{a,s,t}}(\xi_1,\xi_2)\,d\xi_1\,d\xi_2 \\
&= \frac{1}{2\pi i}\int_{\mathbb{R}^2} \hat{H}(\xi_1,\xi_2)\,\partial_1\overline{\hat{\psi}_{a,s,t}}(\xi_1,\xi_2)\,d\xi_1\,d\xi_2 \\
&= \int_{\mathbb{R}^2} \frac{\delta_2(\xi_1,\xi_2)}{2\pi i\xi_1}\,\partial_1\overline{\hat{\psi}_{a,s,t}}(\xi_1,\xi_2)\,d\xi_1\,d\xi_2 \\
&= \int_{\mathbb{R}} \frac{1}{2\pi i\xi_1}\,\partial_1\overline{\hat{\psi}_{a,s,t}}(\xi_1,\xi_2)|_{\xi_2=0}\,d\xi_1 \\
&= a^{\frac{1+\beta}{2}}\overline{\hat{\psi}_2}(a^{\beta-1}s)\int_{\mathbb{R}} \frac{1}{2\pi i\xi_1}\,\partial_1\left(\overline{\hat{\psi}_1}(a\,\xi_1)\,e^{2\pi i\xi_1 t_1}\right)d\xi_1 \\
&= a^{\frac{1+\beta}{2}}\overline{\hat{\psi}_2}(a^{\beta-1}s)\int_{\mathbb{R}} \frac{1}{2\pi i\xi_1}\,\left(a\partial_1\left(\overline{\hat{\psi}_1}\right)(a\,\xi_1) + 2\pi i t_1\overline{\hat{\psi}_1}(a\,\xi_1)\right)e^{2\pi i\xi_1 t_1}\,d\xi_1.
\end{aligned}$$

Similar to the observations from Section 1, under the assumption that $\hat{\psi}_1 \in C_c^\infty(\mathbb{R})$ it follows that $\mathcal{SH}_\psi(x_1H)(a,s,t)$ decays rapidly, asymptotically for $a \to 0$, for all (t_1,t_2) when $t_1 \neq 0$, and for $t_1 = 0$, $s \neq 0$. On the other hand, if $t_1 = 0$ and $s = 0$ we have:

$$\mathcal{SH}_\psi(x_1H)(a,s,t) = a^{\frac{3+\beta}{2}}\overline{\hat{\psi}_2}(0)\int_{\mathbb{R}} \frac{1}{2\pi i\xi_1}\,\partial_1\left(\overline{\hat{\psi}_1}\right)(a\,\xi_1)\,d\xi_1.$$

Provided that $\hat{\psi}_2(0) \neq 0$ and that the integral on the right hand side of the equation above is non-zero, it follows that $\mathcal{SH}_\psi(x_1H)(a,s,t) = O(a^{\frac{3+\beta}{2}})$.

If the ideal ramp edge is replaced by a polynomial-type edge $x_1^m H(x_1,x_2)$, using the same argument above we can show that the continuous shearlet transform will exhibit slow asymptotic decay at the edge location $t_1 = 0$, when $s = 0$, with decay rate $O(a^{\frac{2m+1+\beta}{2}})$. In other words, the example suggests that, also in the case of gen-

eral edges, the continuous shearlet transform may be able to capture the geometry of edge curves through its asymptotic behavior at fine scales.

It was recently shown [22] that it is possible to extend the shearlet-based analysis of edges to general functions of the form $B = f\chi_S$ where $f \in C^\infty(\mathbb{R}^2)$ and $S \subset \mathbb{R}^2$ is a compact region with piecewise smooth boundary ∂S. The analysis of this problem is significantly more involved than the example illustrated above. This is due not only to the fact that, as in the analysis of step edges, there no explicit expression for the Fourier transform of $B = f\chi_S$, but also to the fact that f and its partial derivatives up to an arbitrary order may vanish at ∂S. To deal with this situation, the method proposed in [22] uses a slightly modified shearlet transform. The detailed presentation of this result is beyond the scope of this chapter and we refer the interested reader to the paper. We also recall that other partial results about the analysis of 'general' edges using methods based on the shearlet transform can be found in [17, 24].

Finally, we recall that the microlocal analysis of edges and singularities plays a very significant role in the problem of *geometric separation*, aiming to break up functions or distributions into geometrically distinct components. It was observed by that Donoho and Kutyniok that the ability to achieve such separation is frequently a consequence of the ability to discriminate singularities. As a mathematical idealization of a class of images, they consider distributions of the form $f = P + T$, where P is a collection of point-like singularities and T is a piece-wise smooth function containing curvilinear edges. By expanding f within a combined dictionary of wavelets and curvelets and enforcing sparsity via minimization of the expansion coefficients in the ℓ^1-norm, they proved that the geometric components P and T can be separately recovered by wavelets and curvelets, respectively, asymptotically at fine scales [10]. This result relies on the microlocal properties of wavelets and curvelets. In a recent paper [23], the authors of this chapter proved an extension of the geometric separation result to the three-dimensional setting using the shearlet-based methods presented in Section 4.

5.2 Numerical applications

The mathematical results presented in this chapter about the geometric analysis of singularities in multivariate functions provide the theoretical justification for a number of numerical methods for edge analysis and detection, and for feature extraction in images. We briefly describe below some of these applications.

In particular, a shearlet-based algorithm for edge detection was introduced in [41, 42], based on the properties of the continuous shearlet transform and taking advantage of its ability to accurately detect the edge orientation. This algorithm was shown to be very competitive with respect to more conventional edge detectors and inspired the development of similar directional-sensitive methods. Such methods include an edge detector using anisotropic Gaussian kernels which generate shearlet-like filters [39] and a method using a sort of directional spline wavelets [25]. An extension

of the original shearlet-based algorithm for edge detection to the three-dimensional setting was developed in [38].

The theoretical properties of the continuous shearlet transform also justify a number of numerical methods designed to extract features in images. In particular, the analysis of step edges in Sections 3 shows that corner points are associated with the presence of two directions where the continuous shearlet transform has 'slow' asymptotic decay. This property was exploited in [42] to derive an algorithm to detect corners and other landmarks in images. A refined version of this corner detection algorithm was recently proposed in [11]. More generally, one can derive discrete algorithms based on the continuous shearlet transform to extract geometrical features associated with edges in images. An examples of such applications can be found in [32, 37], where a shearlet-based geometric descriptor called Directional Ratio is introduced to reliably detect morphological properties in fluorescent images of neuronal cultures.

Appendix

We recall some basic facts from Fourier analysis, including the Fourier transform of distributions. We refer the reader to [12, 13] for additional details.

The Fourier transform

$L^1(\mathbb{R}^n)$ is the space of Lebesgue integrable function on $\mathbb{R}^n$ and $L^2(\mathbb{R}^n)$ the Hilbert space of square Lebesgue integrable function on $\mathbb{R}^n$ endowed with the inner product $\langle f,g\rangle = \int_{\mathbb{R}^n} f\overline{g}$. The Schwartz space $\mathscr{S}(\mathbb{R}^n)$ consists of those function in $C^\infty(\mathbb{R}^n)$ which, together with all their derivatives, vanish at infinity faster than any power of $|x|$. That is,

$$\mathscr{S}(\mathbb{R}^n) = \{f \in C^\infty(\mathbb{R}^n) : \sup_{x\in\mathbb{R}^n} (1+|x|)^N |\partial^\alpha f(x)| < \infty, \text{ for all } N, \alpha\},$$

where N is any non negative integer and $\alpha = (\alpha_1, \ldots, \alpha_n)$ is any multi-index.

Definition 1. The *Fourier transform* is the operator $\mathscr{F}$ mapping a function $f \in L^1(\mathbb{R}^n)$ into $\mathscr{F}f = \hat{f}$ defined by

$$\hat{f}(\xi) = \int_{\mathbb{R}^n} f(x) e^{-2\pi i x\cdot\xi} dx.$$

The *inverse Fourier transform* is the operator $\mathscr{F}^{-1}$ mapping a function $g \in L^1(\mathbb{R}^n)$ into $\mathscr{F}^{-1}g = \check{g}$, where

$$\check{g}(x) = \hat{g}(-x) = \int_{\mathbb{R}^n} g(\xi) e^{2\pi i x\cdot\xi} d\xi.$$

It is a fact that $g = (\hat{g})^\vee$ for any function $g \in L^1(\mathbb{R}^n)$ with $\hat{g} \in L^1(\mathbb{R}^n)$.

The Fourier transform is a bijection of $\mathscr{S}$ onto itself and can be extended via an appropriate limit to a unitary map from L^2 onto itself. Under this extension, the Fourier inversion theorem is valid and, for $f, g \in L^2(\mathbb{R}^n)$, the *Plancherel formula* holds:

$$\langle f, g \rangle = \langle \hat{f}, \hat{g} \rangle,$$

and, in particular,

$$\|f\|_2 = \|\hat{f}\|_2.$$

Among the most important properties of Fourier analysis we recall the following list of results (cf. [12]).

Theorem 5. *Let $f, g \in L^1(\mathbb{R}^n)$.*

(i) $(T_y f)^\wedge(\xi) = e^{-2\pi i \xi \cdot y} \hat{f}(\xi)$ *and* $(D_M f)^\wedge(\xi) = D_N \hat{f}(\xi)$, *where* $N = (M^*)^{-1}$.
(ii) $(f * g)^\wedge = \hat{f}\,\hat{g}$.
(iii) If $x^\alpha f \in L^1$ *for* $|\alpha| \le k$, *then* $\partial^\alpha \hat{f} = ((-2\pi i x)^\alpha f)^\wedge$.
(iv) If $f \in C^k$, $\partial^\alpha \hat{f} \in L^1$, *for* $|\alpha| \le k$, *and* $\partial^\alpha \hat{f} \in C_0$, *for* $|\alpha| \le k-1$, *then* $(\partial^\alpha \hat{f})^\wedge(\xi) = (2\pi i \xi)^\alpha \hat{f}(\xi)$.
(v) $\mathscr{F}\left(L^1(\mathbb{R}^n)\right) \subset C_0(\mathbb{R}^n)$.

The following proposition is a simple application of the Fourier transform showing that regularity on $\mathbb{R}^n$ implies decay in the Fourier domain.

Proposition 4. *Suppose that $\psi \in L^2(\mathbb{R}^n)$ is such that $\hat{\psi} \in C_c^\infty(R)$, where $R = \operatorname{supp} \hat{\psi} \subset \mathbb{R}^n$. Then, for each $k \in \mathbb{N}$, there is a constant $C_k > 0$ such that, for any $x \in \mathbb{R}^n$, we have*

$$|\psi(x)| \le C_k \, (1 + |x|^2)^{-k}.$$

In particular, $C_k = k\, m(R) \left(\|\hat{\psi}\|_\infty + \|\triangle^k \hat{\psi}\|_\infty \right)$, where $\triangle = \sum_{i=1}^n \frac{\partial^2}{\partial \xi_i^2}$ is the Fourier-domain Laplacian operator and $m(R)$ is the Lebesgue measure of R.

Proof. From the definition of the Fourier transform, it follows that, for every $x \in \mathbb{R}^n$,

$$|\psi(x)| \le m(R) \, \|\hat{\psi}\|_\infty. \tag{19}$$

An integration by parts shows that

$$\int_R \triangle \hat{\psi}(\xi) \, e^{2\pi i \langle \xi, x \rangle} \, d\xi = -(2\pi)^2 \, |x|^2 \, \psi(x).$$

Thus, for every $x \in \mathbb{R}^n$,

$$(2\pi \, |x|)^{2k} \, |\psi(x)| \le m(R) \, \|\triangle^k \hat{\psi}\|_\infty. \tag{20}$$

Using (19) and (20), we have

$$\left(1 + (2\pi \, |x|)^{2k}\right) |\psi(x)| \le m(R) \left(\|\hat{\psi}\|_\infty + \|\triangle^k \hat{\psi}\|_\infty \right). \tag{21}$$

Observe that, for each $k \in \mathbb{N}$,

$$(1+|x|^2)^k \leq \left(1+(2\pi)^2|x|^2\right)^k \leq k\left(1+(2\pi|x|)^{2k}\right).$$

Using this last inequality and (21), we have that for each $x \in \mathbb{R}^n$

$$|\psi(x)| \leq k\, m(R)\,(1+|x|^2)^{-k}\left(\|\hat{\psi}\|_\infty + \|\triangle^k \hat{\psi}\|_\infty\right). \quad \square$$

Under the same assumptions of Proposition 4, we can derive a similar estimate valid for $\psi_{M,t} = T_t D_M \psi$. Using a change of variable in the last step of the proof above, we have that for all $k > 0$ there is a $C_k > 0$ such that

$$|\psi_{M,t}(x)| \leq C_k\, |\det M|^{-\frac{1}{2}}\,(1+|M^{-1}(x-t)|^2)^{-k}.$$

Distributions and the Fourier transform of distributions

The space $\mathscr{D}(\mathbb{R}^n)$ of *test functions* is the space of all C^∞ functions whose support is compact. A sequence $\{\phi_j\}$ in $\mathscr{D}(\mathbb{R}^n)$ converges in $\mathscr{D}$ to ϕ if the supports of all ϕ_j are contained in a fixed compact subset of $\mathbb{R}^n$ and if $\partial^\alpha \phi_j \to \partial^\alpha \phi$ uniformly for all multi-indices α.

Definition 2. A *distribution* is a continuous linear functional on $\mathscr{D}$ and the space of distributions is denoted by $\mathscr{D}'$. We impose the weak* topology on $\mathscr{D}'$, that is, the topology of pointwise convergence on $\mathscr{D}$.

If $F \in \mathscr{D}'(\mathbb{R}^n)$ and $\phi \in \mathscr{D}(\mathbb{R}^n)$, we denote the value of F at ϕ by $F(\phi)$ or $\langle F, \phi\rangle$. The latter notation conflicts with the notation of inner product but its meaning will be clear by the context.

Given two distribution F and G, we say that $F = G$ is $\langle F, \phi\rangle = \langle G, \phi\rangle$, for all $\phi \in \mathscr{D}(\mathbb{R}^n)$.

Example 1. Every $f \in L^1_{loc}(\mathbb{R}^n)$ defines a distribution by $\phi \in \mathscr{S}(\mathbb{R}^n) \to \int_{\mathbb{R}^n} f\phi$.

Example 2. The *Dirac's impulse* δ is defined by $\delta(\phi) = \langle \delta, \phi\rangle = \phi(0)$, $\phi \in \mathscr{S}(\mathbb{R}^n)$. This is an example of a distribution which is not a function.

Example 3. The distribution $\mathrm{pv}(\frac{1}{x})$ is defined by

$$\langle \mathrm{pv}(\tfrac{1}{x}), \phi\rangle = P.V. \int_{\mathbb{R}} \frac{\phi(x)}{x}\, dx = \lim_{\varepsilon \to 0} \int_{-\varepsilon}^{\varepsilon} \frac{\phi(x)}{x}\, dx,$$

for $\phi \in \mathscr{S}(\mathbb{R})$, where P.V. is the principal value of the integral.

There is a general procedure for extending many linear operations from functions to distributions.

- *Differentiation.* For any $F \in \mathscr{D}'(\mathbb{R}^n)$, the derivatives $\partial^\alpha F \in \mathscr{D}'(\mathbb{R}^n)$ are given by

$$\langle \partial^\alpha F, \phi \rangle = (-1)^{|\alpha|} \langle F, \partial^\alpha \phi \rangle.$$

- *Multiplication by a smooth function.* Given $g \in C^\infty(\mathbb{R}^n)$, for any $F \in \mathscr{D}'(\mathbb{R}^n)$, the product $gF \in \mathscr{D}'(\mathbb{R}^n)$ is given by

$$\langle gF, \phi \rangle = \langle F, g\phi \rangle.$$

- *Convolution.* Let $g \in C^\infty(\mathbb{R}^n)$. For any $F \in \mathscr{D}'(\mathbb{R}^n)$, the convolution $F * g \in \mathscr{D}'(\mathbb{R}^n)$ is given by

$$\langle F * g, \phi \rangle = \langle F, \phi * \tilde{g} \rangle,$$

where $\tilde{g}(x) = g(-x)$.

For example, let H be the one-dimensional Heaviside function, defined by $H(x) = 0$ if $x < 0$, $H(x) = 1$ if $x \geq 0$. A direct computation shows that, for any $\phi \in \mathscr{S}(\mathbb{R})$,

$$\langle H', \phi \rangle = -\langle H, \phi' \rangle = -\int_0^\infty \phi'(x)\, dx = \phi(0) = \langle \delta, \phi \rangle.$$

Hence $H' = \delta$.

The following class of distributions are useful to extend the Fourier transform beyond the realm of classical functions.

Definition 3. A *tempered distribution* is a continuous linear functional on $\mathscr{S}$ and the space of tempered distributions is denoted by $\mathscr{S}'$. We impose the weak* topology on $\mathscr{S}'$, that is, the topology of pointwise convergence on $\mathscr{S}$.

Example 4. Every $f \in L^1_{loc}(\mathbb{R}^n)$ such that $\int_{\mathbb{R}^n} (1+|x|)^N |f(x)|\, dx < \infty$ defines a tempered distribution by $\phi \to \int f\phi$.

Example 5. Any distribution with compact support is tempered.

The Fourier transform extends to a continuous linear map from $\mathscr{S}'$ to itself by defining

$$\langle \hat{F}, \phi \rangle = \langle F, \hat{\phi} \rangle, \quad F \in \mathscr{S}', \phi \in \mathscr{S}.$$

This definition agrees with the classical definition when $F \in L^1 \cap L^2$. Furthermore, it is easy to verify that the basic properties of the Fourier transform continue to hold. In particular, for $F \in \mathscr{S}'(\mathbb{R}^n)$, we have the following formulas.

(i) $(T_y F)^\wedge = e^{-2\pi i \xi \cdot y} \hat{F}$ and $(D_M F)^\wedge = D_N \hat{F}$, where $N = (M^*)^{-1}$.
(ii) $(F * g)^\wedge = \hat{F}\, \hat{g}$, for $g \in \mathscr{S}(\mathbb{R}^n)$.
(iii) $\partial^\alpha \hat{F} = ((-2\pi i x)^\alpha F)^\wedge$.
(iv) $(\partial^\alpha \hat{F})^\wedge = (2\pi i \xi)^\alpha \hat{F}$.

Similarly, the inverse Fourier transform is defined on $\mathscr{S}'$ by

$$\langle \check{F}, \phi \rangle = \langle F, \check{\phi} \rangle, \quad F \in \mathscr{S}', \phi \in \mathscr{S},$$

and, for all $F \in \mathscr{S}'(\mathbb{R}^n)$, $F = (\check{F})^{\wedge} = (\hat{F})^{\vee}$.

Example 6. For any $\phi \in \mathscr{S}(\mathbb{R})$,

$$\langle \hat{\delta}, \phi \rangle = \langle \delta, \hat{\phi} \rangle = \hat{\phi}(0) = \int_{\mathbb{R}} \phi(x)\, dx = \langle 1, \phi \rangle.$$

Hence $\hat{\delta} = 1$. It follows that, for any $y \in \mathbb{R}$, the Fourier transform of $\delta_y = T_y \delta$ is $\hat{\delta}_y(\xi) = e^{-2\pi i y \xi}$ and, for any $k \in \mathbb{N}$, $\widehat{\delta^{(k)}}(\xi) = (2\pi i \xi)^k$.

Example 7. We will show that $\widehat{\mathrm{sgn}}(\xi) = \frac{1}{i\pi}\mathrm{pv}(\frac{1}{\xi})$, where sgn is the *signum* function, that is defined as $\mathrm{sgn}(x) = -1$ of $x < 0$, $\mathrm{sgn}(x) = 0$ of $x \geq 0$. In order to derive this result, we consider first the functions f_n defined by $f_n(x) = \begin{cases} -e^{x/n} & \text{if } x < 0 \\ e^{-x/n} & \text{if } x > 0 \end{cases}$, where $n \in \mathbb{N}$. An application of Lebesgue Dominated Convergence theorem shows that f_n converges to $f = \mathrm{sgn}$ as $n \to \infty$ in the sense of tempered distributions, that is, $\langle f_n, \phi \rangle \to \langle \mathrm{sgn}, \phi \rangle$ as $n \to \infty$, for all $\phi \in \mathscr{S}(\mathbb{R})$. A direct computation (note that $f_n \in L^1(\mathbb{R})$) shows that

$$\hat{f}_n(\xi) = \int_0^{\infty} e^{-x/n} e^{-2\pi i x \xi}\, dx - \int_{-\infty}^{0} e^{x/n} e^{-2\pi i x \xi}\, dx = \frac{1}{\frac{1}{n} + 2\pi i \xi} - \frac{1}{\frac{1}{n} - 2\pi i \xi}.$$

Finally, we use that fact that if $(F_n), F \in \mathscr{S}'$ and $\langle F_n, \phi \rangle \to \langle F, \phi \rangle$ for all $\phi \in \mathscr{S}$, then $\langle \hat{F}_n, \phi \rangle \to \langle \hat{F}, \phi \rangle$ for all $\phi \in \mathscr{S}$. Since

$$\lim_{n \to \infty} \langle \hat{f}_n, \phi \rangle = \frac{1}{i\pi} P.V. \int \frac{\phi(\xi)}{\xi} d\xi,$$

we conclude that $\widehat{\mathrm{sgn}}(\xi) = \frac{1}{i\pi}\mathrm{pv}(\frac{1}{\xi})$.

Example 8. The one-dimensional Heaviside function $H(x)$ can be written as $H(x) = \frac{1}{2} + \frac{1}{2}\mathrm{sgn}(x)$. It follows that $\hat{H}(\xi) = \frac{1}{2}\delta(\xi) + \frac{1}{2\pi i}\mathrm{pv}(\frac{1}{\xi})$.

Example 9. Let us consider the two-dimensional Heaviside function $H_1(x_1, x_2) = \chi_{x_1 > 0}(x_1, x_2)$. Since it can be written as the tensor product $H_1(x_1, x_2) = H(x_1)1(x_2)$, it follows that $\hat{H}_1(\xi_1, \xi_2) = \frac{1}{2}\delta(\xi_1)\delta(\xi_2) + \frac{\delta(\xi_1)}{2\pi i}\mathrm{pv}(\frac{1}{\xi}_1)$.

Singular support and wavefront set

The notion of singular support is introduced to describe the location where a distribution fails to be smooth. Since a distribution is not defined at a single point, this definition requires to deal with open sets containing the point of interest.

For a distribution F, we say that $x_0 \in \mathbb{R}^n$ is a *regular point* of F if there exists a function $g \in C^\infty(U)$, where $U \subset \mathbb{R}^n$ is an open neighbourhood of x_0 and $g(x_0) = 1$, such that $gF \in C^\infty(U)$. The complement of the set of the regular points of F is called the *singular support* of F and is denoted by $\operatorname{sing\,supp}(F)$. It is easy to see that the singular support of F is a closed set.

For example, $\operatorname{sing\,supp}(\delta) = \{0\}$. Also $\operatorname{sing\,supp}(\operatorname{pv}(\frac{1}{x})) = \{0\}$.

Note that the condition $gF \in C^\infty(U)$ is equivalent to $(gF)^\wedge$ being rapidly decreasing, i.e., for all $N > 0$ there exists a $C_N > 0$ such that

$$(gF)^\wedge(\xi)| \leq C_N (1 + |\xi|)^{-N}.$$

If a function or distribution fails to be smooth, we can look not only for the location of the singularity in space, but also for the orientation of the singularity.

We shall say that a set $\Gamma \in \mathbb{R}^n \setminus \{0\}$ is conic if $\xi \in \Gamma$ implies that $\lambda\xi \in \Gamma$ for all $\lambda > 0$. A *conic neighbourhood* of a point is an open conic set containing it. For a distribution F, the point $(x, \xi) \in \mathbb{R}^n \times \mathbb{R}^n \setminus \{0\}$ is a *regular directed point* of F if there exists a function $g \in C^\infty(U)$, where $U \subset \mathbb{R}^n$ is an open neighbourhood of x and $g(x) = 1$, such that $gF \in C^\infty(U)$ and, for al $N > 0$, there exists a $C_N > 0$ such that

$$|(gF)^\wedge(\xi)| \leq C_N (1 + |\xi|)^{-N},$$

for all ξ is a conic neighbourhood containing the direction ξ_0. The complement in $\mathbb{R}^n \times \mathbb{R}^n \setminus \{0\}$ of the set of regular directed points of F is called the *wavefront set* of F ans is denoted by $WF(F)$.

Example 10. Let $x = (x', x'')$ be a splitting of the coordinates and define the distribution F by

$$\langle F, \phi \rangle = \int \phi(0, x'')\, dx''.$$

It is easy to see that $\operatorname{sing\,supp}(F) = \{(x', x'') : x' = 0\}$. To compute the wavefront set, observe that, for $\gamma \in C^\infty(U)$, where U is a neighbourhood of a point $x_0 = (x_0', x_0'')$, we have:

$$\langle \gamma F, \phi \rangle = \int \gamma(0, x'')\, \phi(0, x'')\, dx''.$$

Thus, $(\gamma F)^\wedge(\xi) = \hat{\gamma}_0(\xi'')$, where $\gamma_0(x'') = \gamma(0, x'')$. Since γ_0 is C^∞ and compactly supported, its Fourier transform has rapid decay as a funxtion of ξ'' but is constant as a function of ξ'. Hence we conclude that $WF(F) = \{(0, x'', \xi', 0)\}$.

Acknowledgements The authors are partially supported by NSF grant DMS 1008900/1008907. DL is also partially supported by NSF grant DMS 1005799.

References

1. J. Bros and D. Iagolnitzer. Support essentiel et structure analytique des distributions. *Seminaire Goulaouic-Lions-Schwartz*, 19, 1975-76.
2. A. Calderòn. Intermediate spaces and interpolation, the complex method. *Studia Mathematica*, 24(2):113–190, 1964.
3. E. J. Candès and D. L. Donoho. New tight frames of curvelets and optimal representations of objects with piecewise C^2 singularities. *Commun. Pure Appl. Anal.*, 57(2):219–266, 2004.
4. E. J. Candès and D. L. Donoho. Continuous curvelet transform: I. resolution of the wavefront set. *Appl. Comp. Harm. Analysis*, 19:162–197, 2005.
5. A. Córdoba and C. Fefferman. Wave packets and fourier integral operators. *Communications in Partial Differential Equations*, 3(11):979–1005, 1978.
6. S. Dahlke, F. De Mari, E. De Vito, S. Häuser, G. Steidl, and G. Teschke. Different faces of the shearlet group. *ArXiv*, (1404.4545), 2014.
7. S. Dahlke, G. Kutyniok, P. Maass, C. Sagiv, H. Stark, and G. Teschke. The uncertainty principle associated with the continuous shearlet transform. *IJWMIP*, 6(2):157–181, 2008.
8. S. Dahlke, G. Steidl, and G. Teschke. The continuous shearlet transform in arbitrary space dimensions. *Journal of Fourier Analysis and Applications*, 16(3):340–364, 2010.
9. J.M. Delort. *F.B.I. transformation: second microlocalization and semilinear caustics*, volume 1522 of *Lecture Notes in Mathematics*. Springer Berlin Heidelberg, 1992.
10. D. L. Donoho and G. Kutyniok. *Commun. Pure Appl. Math.*, 66(1):1–47, 2013.
11. M.A. Duval-Poo, F. Odone, and E. De Vito. Edges and corners with shearlets. *preprint*, 2015.
12. G. B. Folland. *Real analysis*. Pure and Applied Mathematics (New York). John Wiley & Sons, Inc., New York, second edition, 1999. Modern techniques and their applications, A Wiley-Interscience Publication.
13. G. Friedlander and M. Joshi. *Introduction to The Theory of Distributions*. Cambridge University Press, New York, second edition, 1998.
14. P. Gérard. Moyennisation et regularité deux-microlocale. *Ann. Scient. Ec. Norm. Sup., 4eme serie*, 23:89–121, 1990.
15. P Grohs. Continuous shearlet frames and resolution of the wavefront set. *Monatshefte fr Mathematik*, 164(4):393–426, 2011.
16. A. Grossmann. Wavelet transforms and edge detection. In Sergio Albeverio, Philip Blanchard, Michiel Hazewinkel, and Ludwig Streit, editors, *Stochastic Processes in Physics and Engineering*, volume 42 of *Mathematics and Its Applications*, pages 149–157. Springer Netherlands, 1988.
17. K. Guo, R. Houska, and D. Labate. Microlocal analysis of singularities from directional multiscale representations. In Gregory E. Fasshauer and Larry L. Schumaker, editors, *Approximation Theory XIV: San Antonio 2013*, volume 83 of *Springer Proceedings in Mathematics and Statistics*, pages 173–196. Springer International Publishing, 2014.
18. K. Guo and D. Labate. Optimally sparse multidimensional representation using shearlets. *SIAM J. Math. Analysis*, 39(1):298–318, 2007.
19. K. Guo and D. Labate. Characterization and analysis of edges using the continuous shearlet transform. *SIAM J. Imaging Sciences*, 2(3):959–986, 2009.
20. K. Guo and D. Labate. Analysis and detection of surface discontinuities using the 3d continuous shearlet transform. *Appl. Comput. Harmon. Anal.*, 30:231–242, 2010.
21. K. Guo and D. Labate. Characterization of piecewise smooth surfaces using the 3d continuous shearlet transform. *J. Fourier Anal. Appl.*, 18:488–516, 2012.
22. K. Guo and D. Labate. Characterization and analysis of edges in piecewise smooth functions. *preprint*, 2015.
23. K. Guo and D. Labate. Geometric separation of singularities using combined multiscale dictionaries. *J. Fourier Anal. Appl. (in press)*, 2015.
24. K. Guo, D. Labate, and W. Lim. Edge analysis and identification using the continuous shearlet transform. *Appl. Comput. Harmon. Anal.*, 27(1):24–46, 2009.

25. W. Guo and M. Lai. Box spline wavelet frames for image edge analysis. *SIAM Journal on Imaging Sciences*, 6(3):1553–1578, 2013.
26. C. S. Herz. Fourier transforms related to convex sets. *Ann. of Math.*, (75), 1962.
27. M. Holschneider. *Wavelets. Analysis tool*. Oxford University Press, Oxford, 1995.
28. R. Houska and D. Labate. Detection of boundary curves on the piecewise smooth boundary surface of three dimensional solids. *Appl. Comput. Harmon. Anal.*, 2014.
29. S. Jaffard. Pointwise smoothness, two-microlocalization and wavelet coefficients. *Publicacions Matemàtiques*, 35(1):155–168, 1991.
30. S. Jaffard and Y. Meyer. Wavelet Methods for Pointwise Regularity and Local Oscillations of Functions. *Mem. Amer. Math. Soc.*, 123, September 1996.
31. G. Kutyniok and D. Labate. Resolution of the wavefront set using continuous shearlets. *Trans. Am. Math. Soc.*, 361(5):2719–2754, 2009.
32. D. Labate, F. Laezza, P. Negi, B. Ozcan, and M. Papadakis. Efficient processing of fluorescence images using directional multiscale representations. *Math. Model. Nat. Phenom.*, 9(5):177–193, 2014.
33. R.S. Laugesen, N. Weaver, G.L. Weiss, and E.N. Wilson. A characterization of the higher dimensional groups associated with continuous wavelets. *The Journal of Geometric Analysis*, 12(1):89–102, 2002.
34. D. Marr. Early processing of visual information. *Phil. Trans. R. Soc. Lond. B*, 275:483–524, 1976.
35. D. Marr and E. Hildreth. Theory of Edge Detection. *Proceedings of the Royal Society of London. Series B, Biological Sciences*, 207(1167):187–217, 1980.
36. Y. Meyer. *Ondelettes et Opérateurs*. Hermann, Paris, 1990.
37. B. Ozcan, D. Labate, D. Jimnez, and M. Papadakis. Directional and non-directional representations for the characterization of neuronal morphology. In *Proc. SPIE. Wavelets XV (San Diego, CA, 2013)*, volume 8858, pages 885803–885803–11, 2013.
38. D.A. Schug, G.R. Easley, and D.P. O'Leary. Three-dimensional shearlet edge analysis. In *Proc. SPIE, Independent Component Analyses, Wavelets, Neural Networks, Biosystems, and Nanoengineering IX*, volume 8058, 2011.
39. P.L. Shui and W.C. Zhang. Noise-robust edge detector combining isotropic and anisotropic gaussian kernels. *Pattern Recogn.*, 45(2):806–820, February 2012.
40. G. Weiss and E.N. Wilson. The mathematical theory of wavelets. In JamesS. Byrnes, editor, *Twentieth Century Harmonic Analysis A Celebration*, volume 33 of *NATO Science Series*, pages 329–366. Springer Netherlands, 2001.
41. S. Yi, D. Labate, G.R. Easley, and H. Krim. Edge detection and processing using shearlets. In *Image Processing, 2008. ICIP 2008. 15th IEEE International Conference on*, pages 1148–1151, Oct 2008.
42. S. Yi, D. Labate, G.R. Easley, and H. Krim. A shearlet approach to edge analysis and detection. *IEEE Transactions on Image Processing*, 18(5):929–941, 2009.
43. D. Ziou and S. Tabbone. Edge detection techniques - an overview. *Int J Pattern Recogn*, 8:537–559, 1998.

Index

admissibility condition, 6
affine group, 5, 6

continuous shearlet transform, 9, 13
continuous wavelet transform, 3, 6
corner point, 15

distribution, 40

edge, 2
  ramp edge, 36
  step edge, 2, 14

FBI transform, 4

geometric separation, 37

Heaviside step function, 2

localization lemma, 19

shearlet group, 8
singular support, 42

wavefront set, 4, 43